US009742960B2

(12) United States Patent
Chen et al.

(10) Patent No.: US 9,742,960 B2
(45) Date of Patent: Aug. 22, 2017

(54) **COLOR CORRECTION SYSTEM AND METHOD**

(71) Applicant: **SZ DJI TECHNOLOGY CO., LTD.**, Shenzhen, Guangdong (CN)

(72) Inventors: **Wei Chen**, Shenzhen (CN); **Zisheng Cao**, Shenzhen (CN)

(73) Assignee: **SZ DJI TECHNOLOGY CO., LTD.**, Shenzhen (CN)

(*) Notice: Subject to any disclaimer, the term of this patent is extended or adjusted under 35 U.S.C. 154(b) by 0 days.

(21) Appl. No.: **15/176,037**

(22) Filed: **Jun. 7, 2016**

(65) **Prior Publication Data**

US 2017/0041507 A1 Feb. 9, 2017

Related U.S. Application Data

(63) Continuation of application No. PCT/CN2015/079094, filed on May 15, 2015.

(51) **Int. Cl.**
G06T 5/00 (2006.01)
H04N 1/60 (2006.01)
(Continued)

(52) **U.S. Cl.**
CPC ***H04N 1/6027*** (2013.01); ***G06T 5/002*** (2013.01); ***G06T 7/0018*** (2013.01); ***G09G 5/02*** (2013.01);
(Continued)

(58) **Field of Classification Search**
CPC H04N 1/6027; G06T 5/002; G06T 7/0018; G06T 2207/10024
See application file for complete search history.

(56) **References Cited**

U.S. PATENT DOCUMENTS

5,471,324 A * 11/1995 Rolleston H04N 1/6033 358/518
2002/0034337 A1* 3/2002 Shekter G06K 9/40 382/275
(Continued)

FOREIGN PATENT DOCUMENTS

CN	1622135	A	1/2015
JP	2008099069	A	4/2008
KR	20100079479	A	7/2010

OTHER PUBLICATIONS

Quan ("Analytical Approach to the Optimal Linear Matrix with Comprehensive Error Metric," SPIE Electronic Imaging Conference, vol. 5292, San Jose, 2004).*
(Continued)

Primary Examiner — Yubin Hung
(74) *Attorney, Agent, or Firm* — Anova Law Group, PLLC

(57) **ABSTRACT**

A system and method for calibrating a digital imaging device for color correction is disclosed. The method comprises obtaining an input color value and a reference color value for each of a plurality of color references, as well as a noise evaluation image having a color noise for evaluating noise reduction, the input color values and reference color values being in a non-linear color space. A plurality of color correction parameters are determined as optimized based on evaluating a fitness function in the non-linear color space. The non-linear color space can be a CIE L*a*b* color space. The fitness function can include a color correction error and a noise amplification metric so as to reduce noise amplification during color correction.

30 Claims, 16 Drawing Sheets

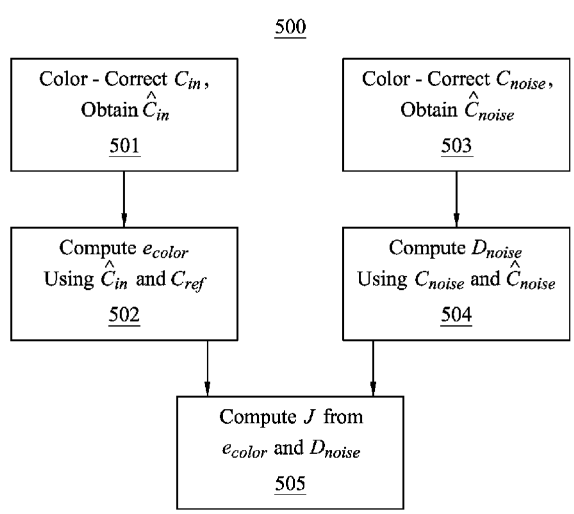

(51) **Int. Cl.**
G09G 5/02 (2006.01)
G09G 5/06 (2006.01)
G06T 7/00 (2017.01)

(52) **U.S. Cl.**
CPC ***G09G 5/06*** (2013.01); *G06T 2207/10024* (2013.01); *G09G 2320/0693* (2013.01); *G09G 2340/0407* (2013.01); *G09G 2340/06* (2013.01); *G09G 2370/12* (2013.01); *G09G 2380/08* (2013.01); *H04N 1/60* (2013.01)

(56) **References Cited**

U.S. PATENT DOCUMENTS

2002/0097907 A1* 7/2002 Fukasawa H04N 1/6058 382/167
2005/0073596 A1* 4/2005 Takahashi H04N 9/045 348/241
2007/0263098 A1* 11/2007 Quan H04N 1/6086 348/222.1
2009/0015674 A1* 1/2009 Alley H04N 7/185 348/144
2013/0016082 A1 1/2013 Coley et al.
2014/0043627 A1 2/2014 Toso et al.
2015/0097990 A1* 4/2015 Manabe H04N 5/23245 348/241
2015/0245002 A1* 8/2015 Kuramoto H04N 9/646 348/70

OTHER PUBLICATIONS

Quan, Shuxue ("Evaluation and optimal design of spectral sensitivities for digital color imaging," Ph.D. Dissertation, College of Science, Rochester Institute of Technology, 2002).*
WO, International Search Report and Written Opinion, PCT/CN2015/079094, Aug. 17, 2015.

* cited by examiner

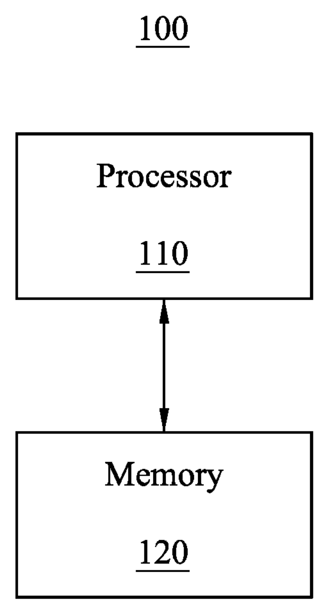

FIG. 1

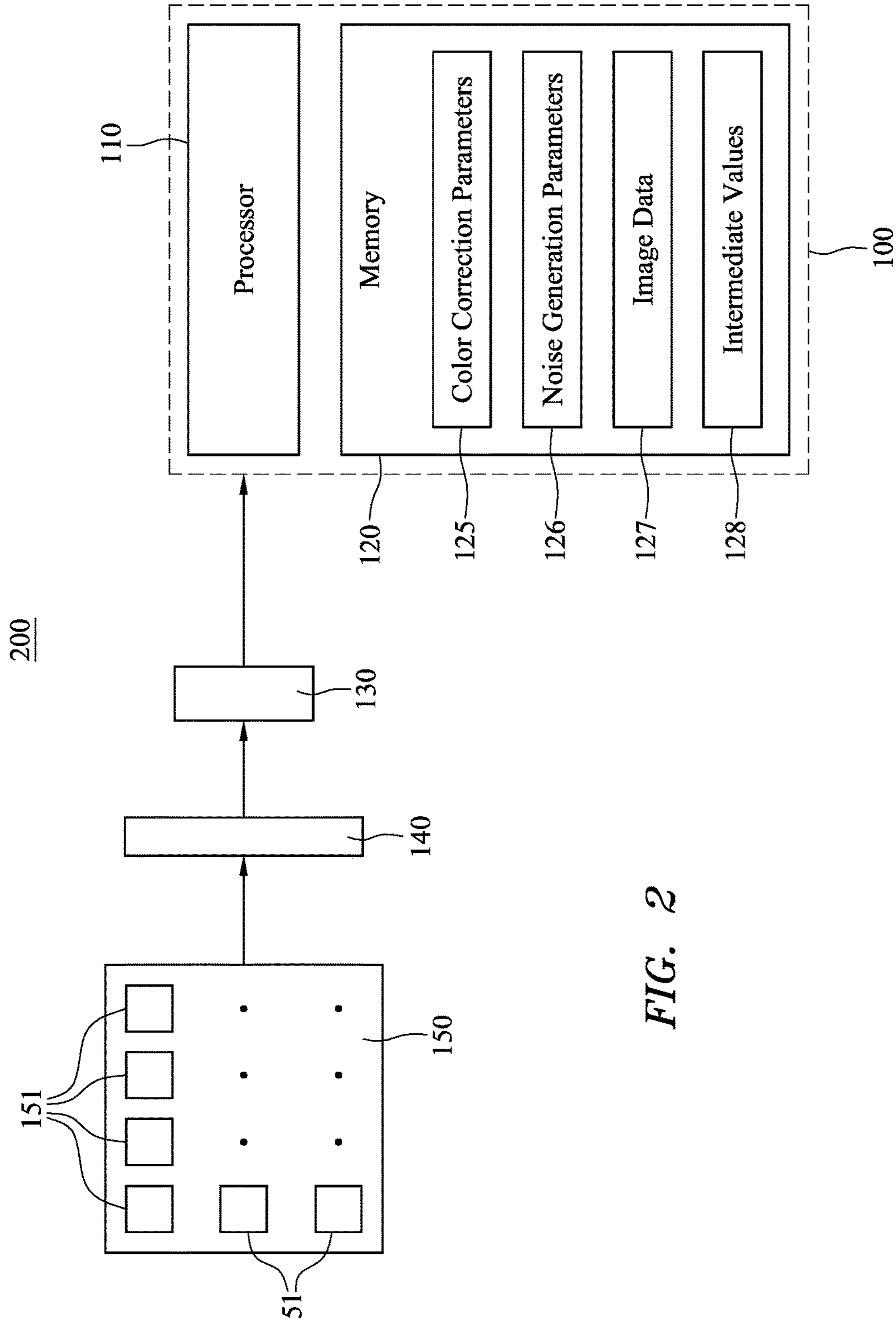
200
110
Processor
Memory
Color Correction Parameters
Noise Generation Parameters
Image Data
Intermediate Values
100
120
125
126
127
128
130
140
150
151
151

FIG. 2

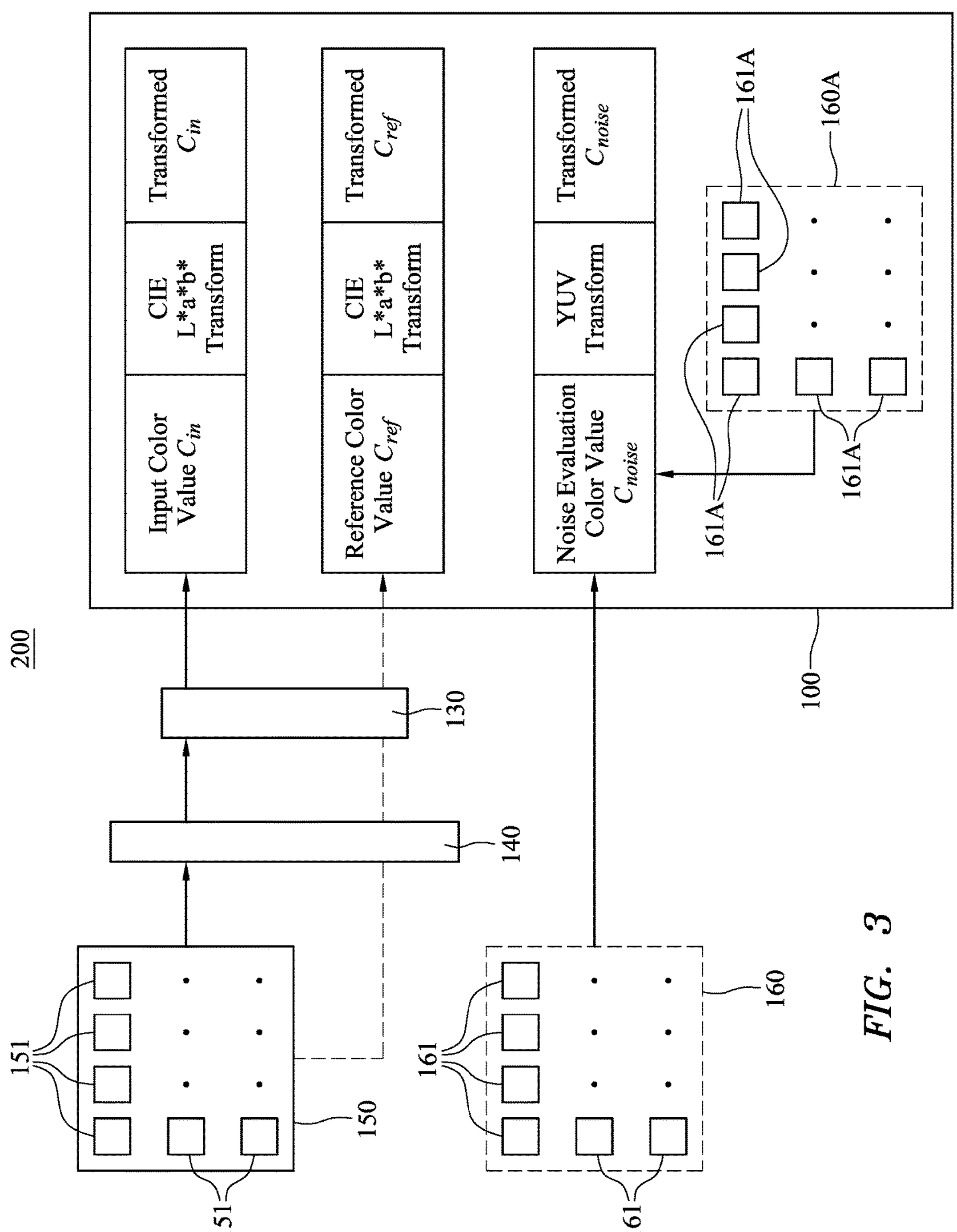
200
Input Color Value C_{in}
CIE L*a*b* Transform
Transformed C_{in}
Reference Color Value C_{ref}
CIE L*a*b* Transform
Transformed C_{ref}
Noise Evaluation Color Value C_{noise}
YUV Transform
Transformed C_{noise}
161A
160A
100
130
140
150
151
160
161

FIG. 3

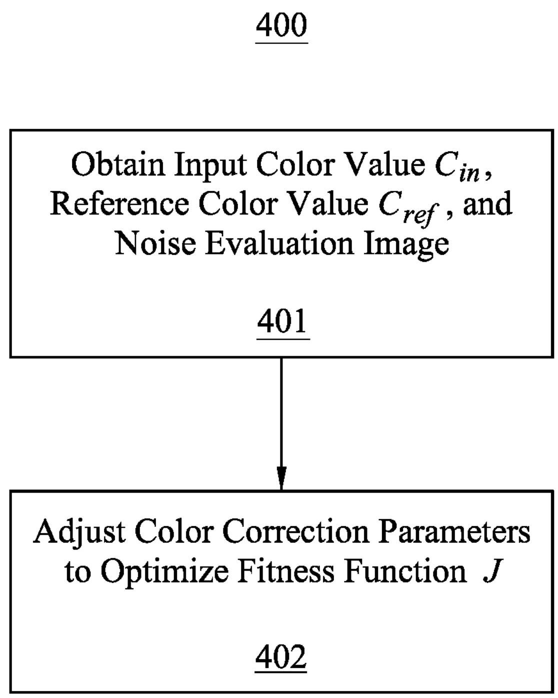
400
Obtain Input Color Value C_{in}, Reference Color Value C_{ref}, and Noise Evaluation Image
401
Adjust Color Correction Parameters to Optimize Fitness Function J
402

FIG. 4

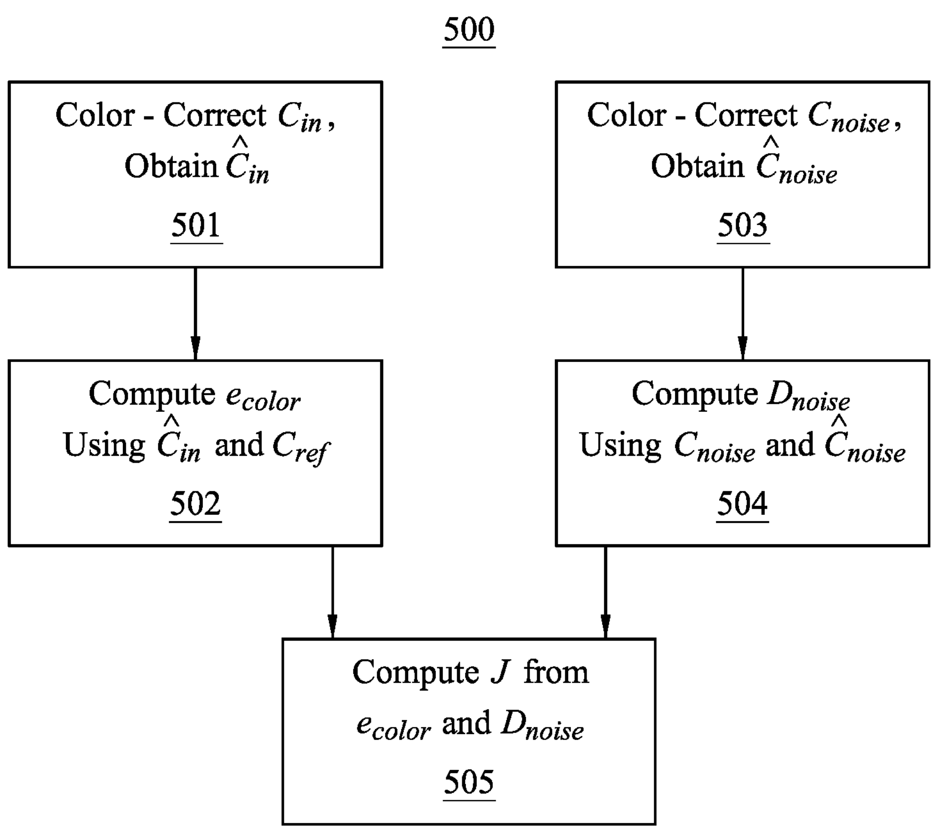
500
Color - Correct C_{in}, Obtain $\hat{C}_{in}$
501
Color - Correct C_{noise}, Obtain $\hat{C}_{noise}$
503
Compute e_{color} Using $\hat{C}_{in}$ and C_{ref}
502
Compute D_{noise} Using C_{noise} and $\hat{C}_{noise}$
504
Compute J from e_{color} and D_{noise}
505

FIG. 5

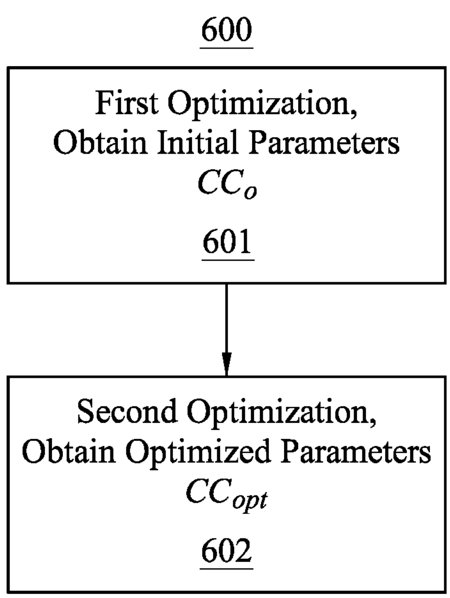
600
First Optimization,
Obtain Initial Parameters
CC_o
601
Second Optimization,
Obtain Optimized Parameters
CC_{opt}
602

FIG. 6

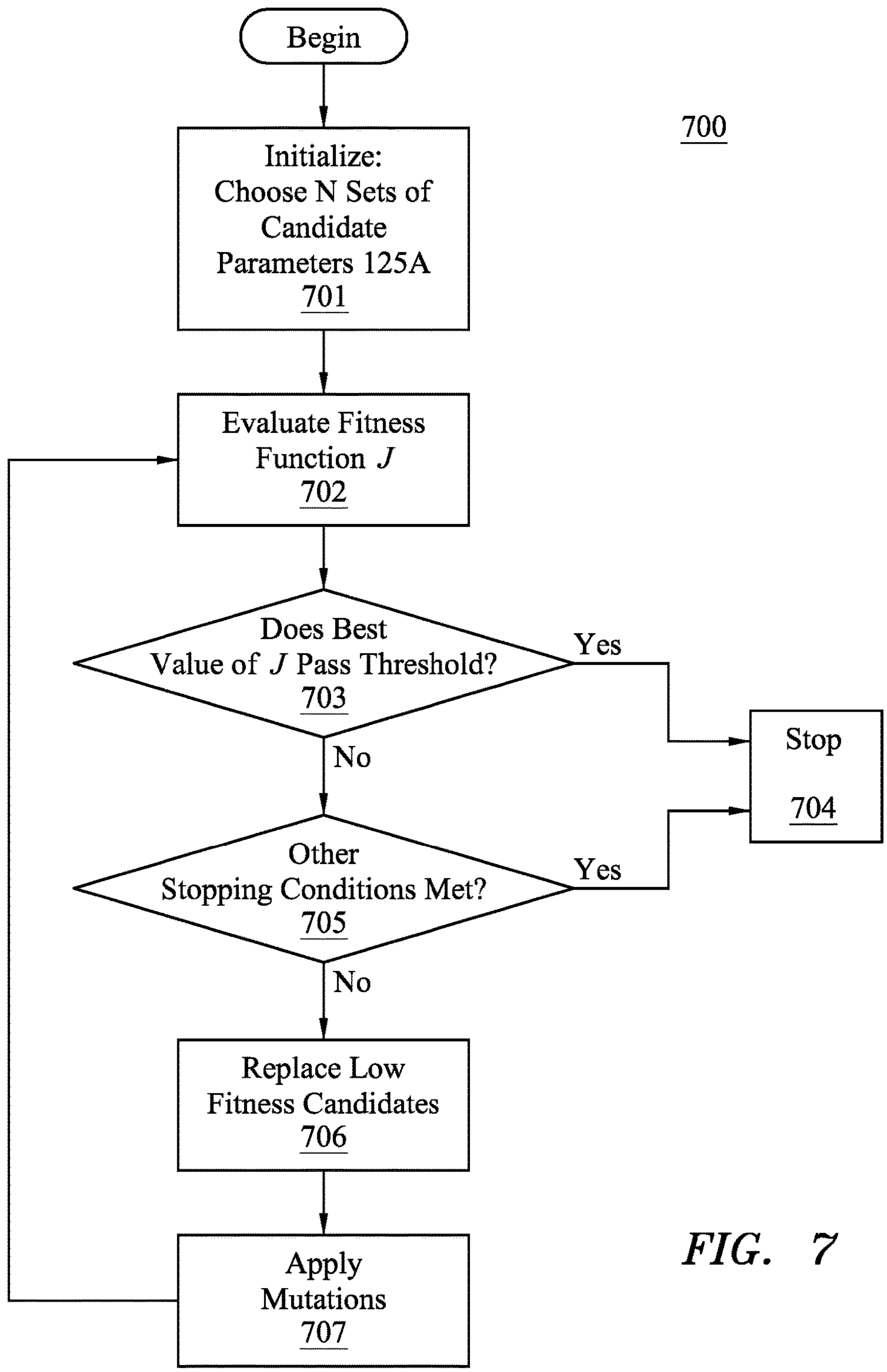
Begin
700
Initialize:
Choose N Sets of
Candidate
Parameters 125A
701
Evaluate Fitness
Function J
702
Does Best
Value of J Pass Threshold?
703
Yes
Stop
704
No
Other
Stopping Conditions Met?
705
Yes
No
Replace Low
Fitness Candidates
706
Apply
Mutations
707

FIG. 7

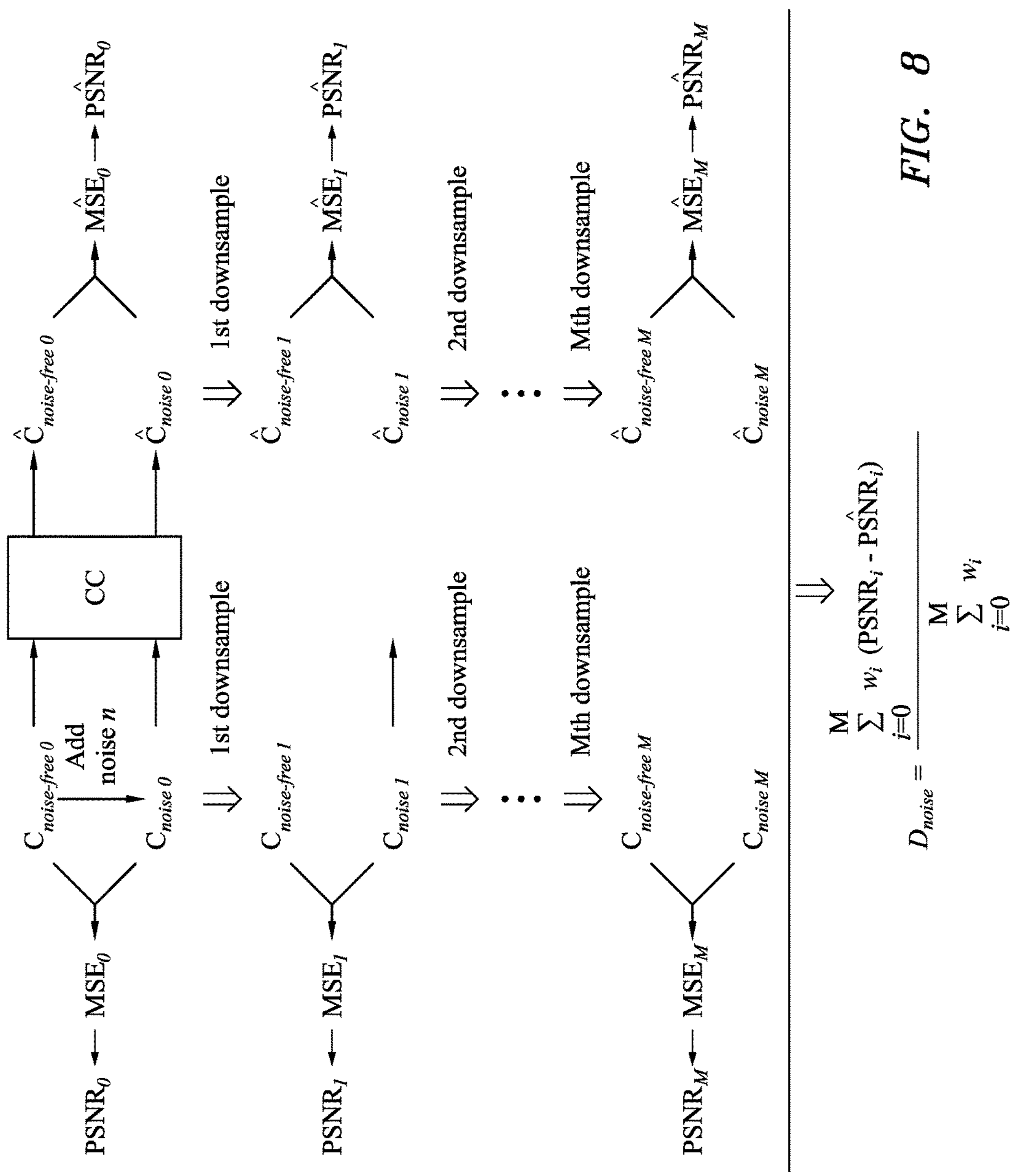
CC
Add noise n
1st downsample
2nd downsample
Mth downsample
$C_{noise\text{-}free\ 0}$
$C_{noise\ 0}$
$\hat{C}_{noise\text{-}free\ 0}$
$\hat{C}_{noise\ 0}$
$PSNR_0 \leftarrow MSE_0$
$\hat{MSE}_0 \rightarrow \hat{PSNR}_0$
$PSNR_1 \leftarrow MSE_1$
$\hat{MSE}_1 \rightarrow \hat{PSNR}_1$
$PSNR_M \leftarrow MSE_M$
$\hat{MSE}_M \rightarrow \hat{PSNR}_M$
$D_{noise} = \frac{\sum_{i=0}^{M} w_i (PSNR_i - \hat{PSNR}_i)}{\sum_{i=0}^{M} w_i}$

FIG. 8

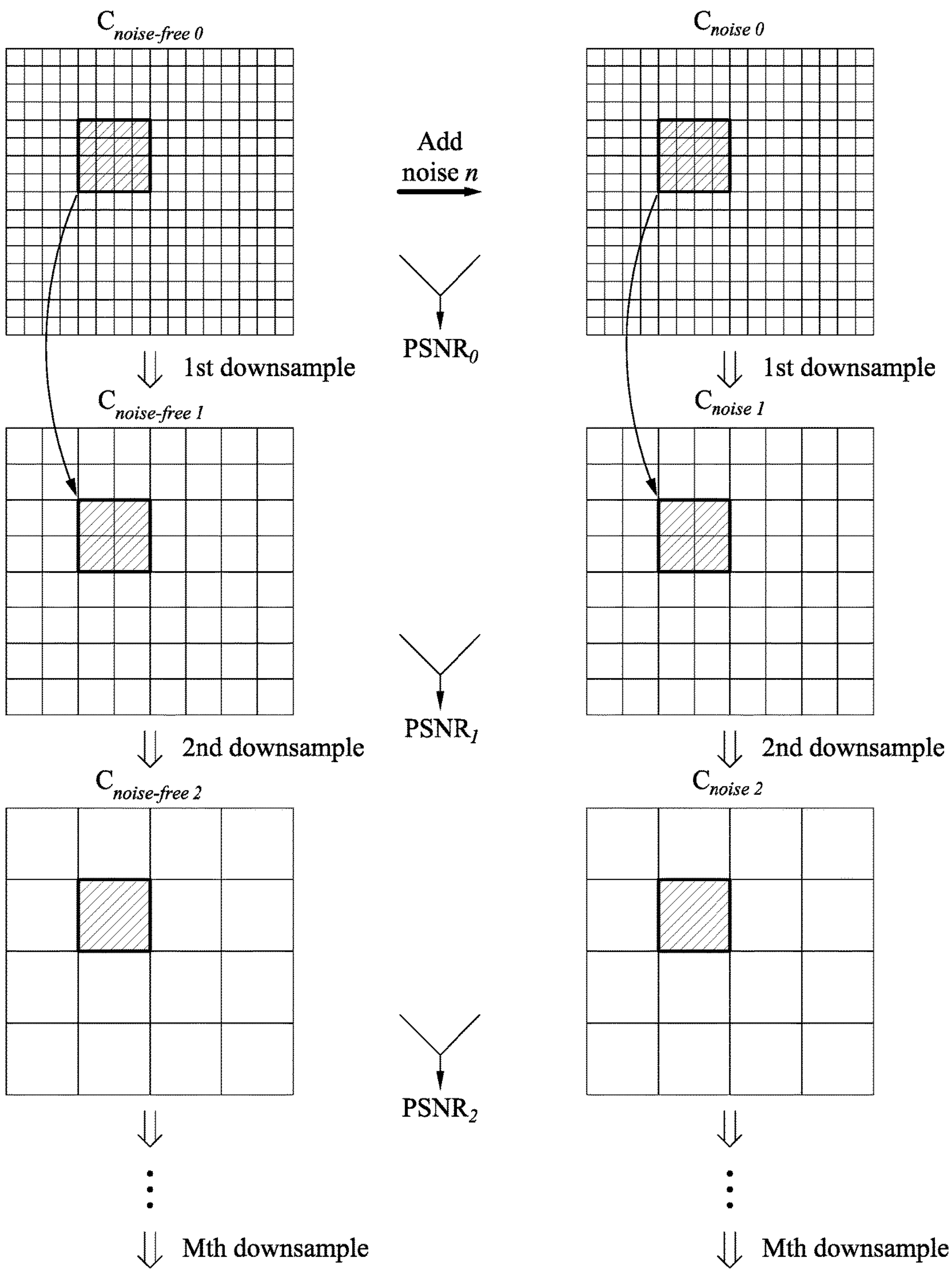
$C_{noise\text{-}free\ 0}$
$C_{noise\ 0}$
Add
noise n
$PSNR_0$
1st downsample
1st downsample
$C_{noise\text{-}free\ 1}$
$C_{noise\ 1}$
$PSNR_1$
2nd downsample
2nd downsample
$C_{noise\text{-}free\ 2}$
$C_{noise\ 2}$
$PSNR_2$
Mth downsample
Mth downsample

FIG. 9

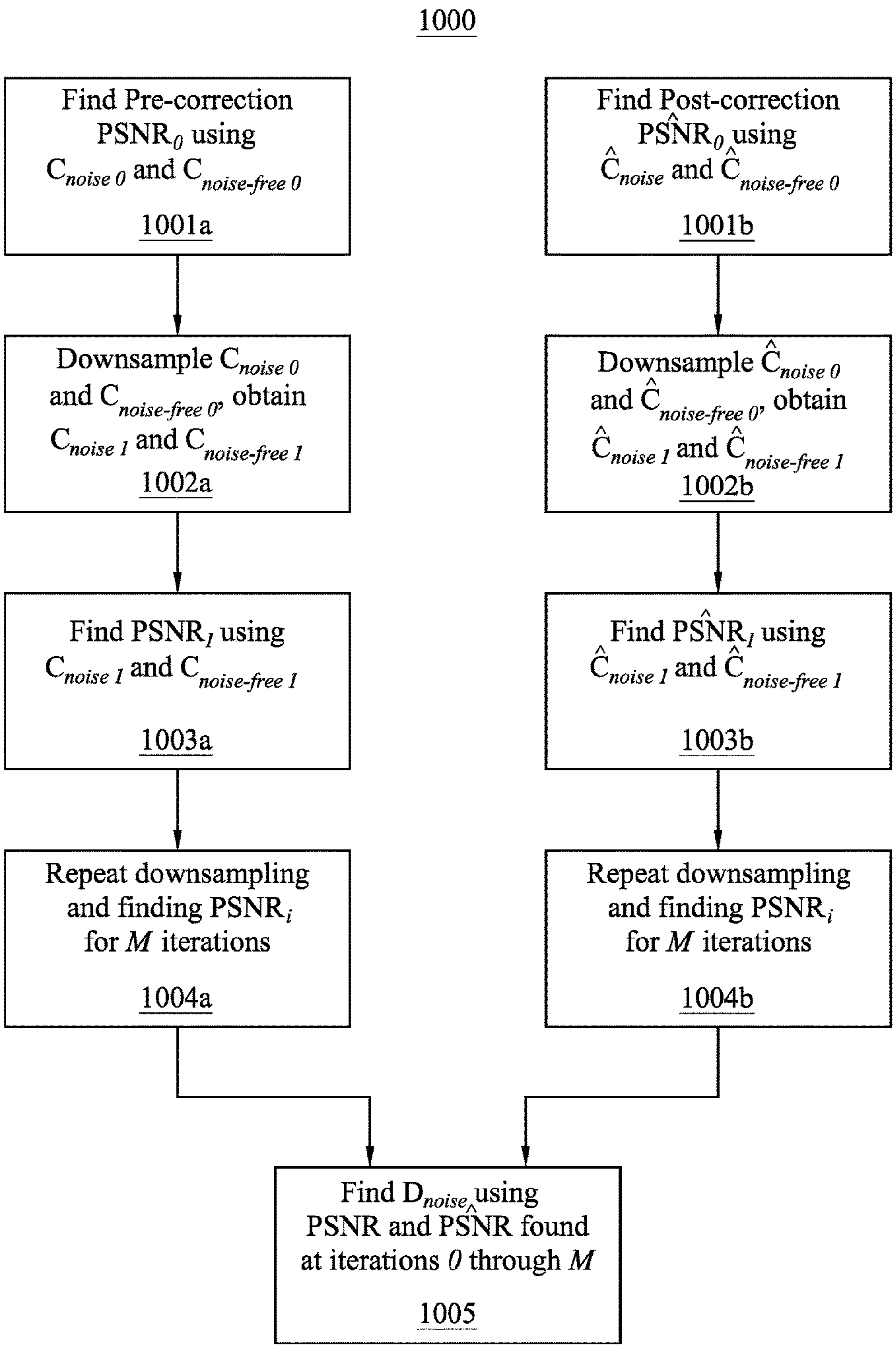
1000
Find Pre-correction PSNR0 using Cnoise 0 and Cnoise-free 0
1001a
Find Post-correction PSNR0 using Ĉnoise and Ĉnoise-free 0
1001b
Downsample Cnoise 0 and Cnoise-free 0, obtain Cnoise 1 and Cnoise-free 1
1002a
Downsample Ĉnoise 0 and Ĉnoise-free 0, obtain Ĉnoise 1 and Ĉnoise-free 1
1002b
Find PSNR1 using Cnoise 1 and Cnoise-free 1
1003a
Find PSNR1 using Ĉnoise 1 and Ĉnoise-free 1
1003b
Repeat downsampling and finding PSNRi for M iterations
1004a
Repeat downsampling and finding PSNRi for M iterations
1004b
Find Dnoise using PSNR and PSNR found at iterations 0 through M
1005

FIG. 10

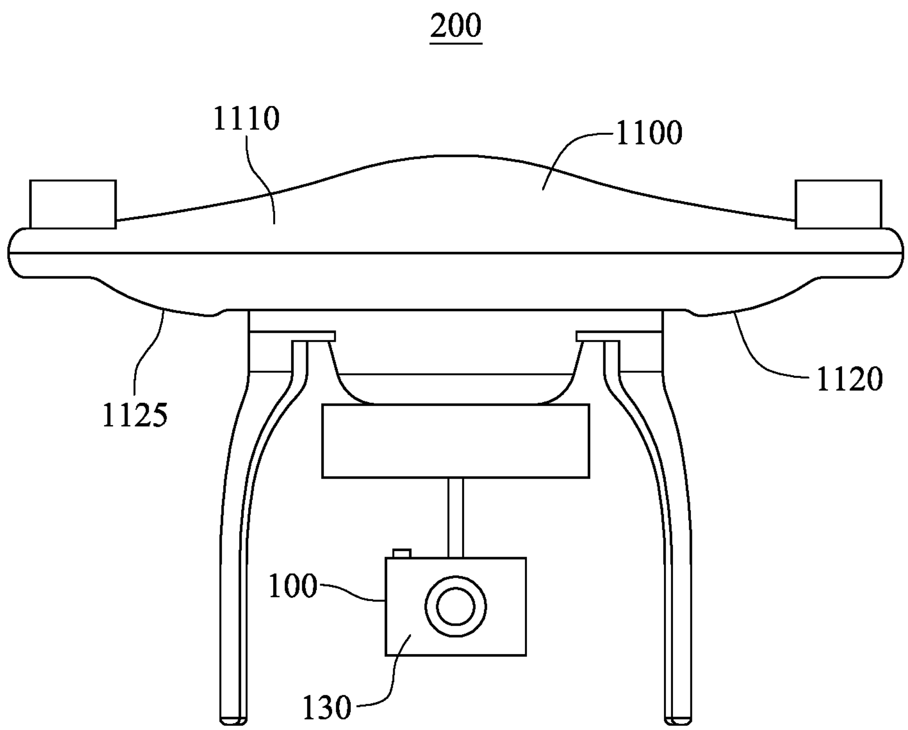

FIG. 11

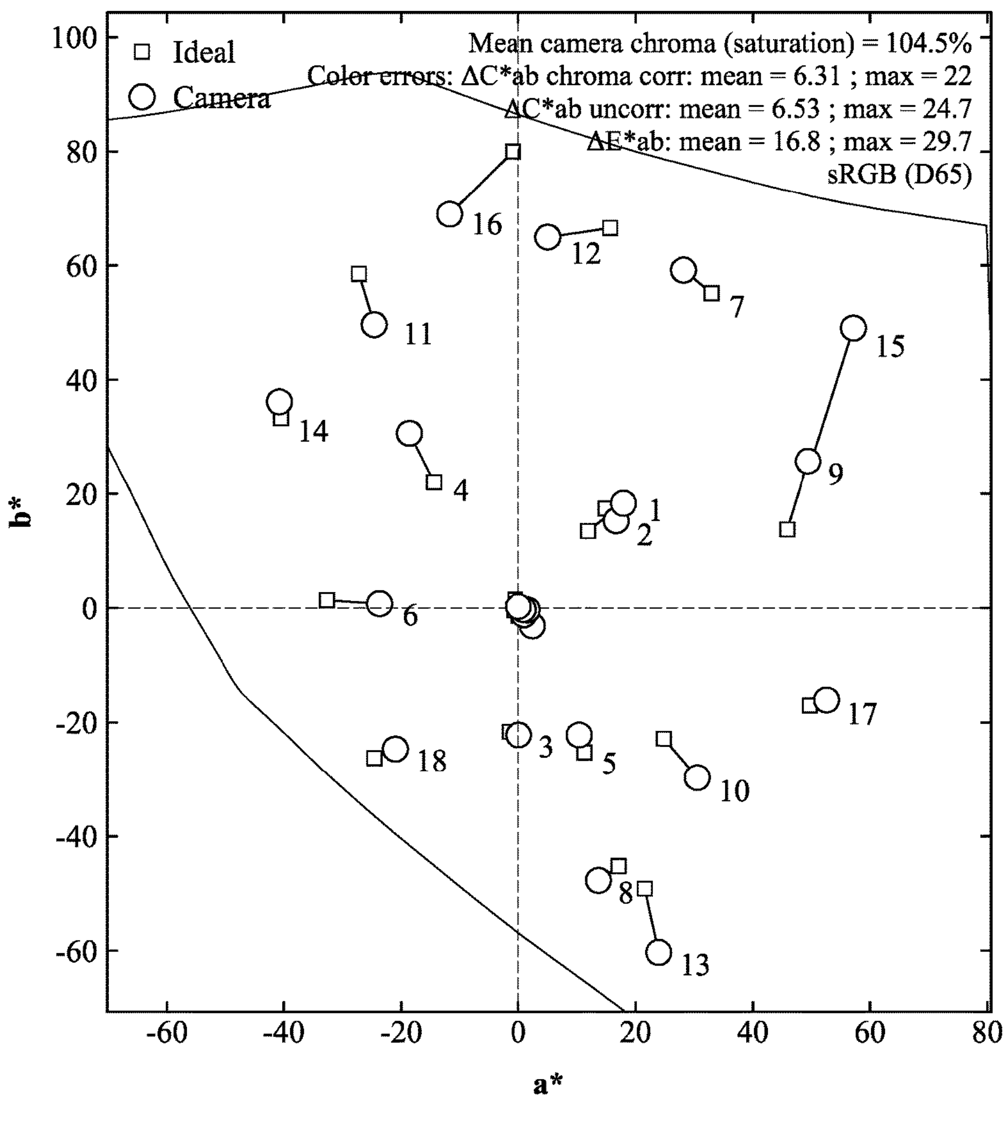
Ideal
Camera
Mean camera chroma (saturation) = 104.5%
Color errors: ΔC*ab chroma corr: mean = 6.31 ; max = 22
ΔC*ab uncorr: mean = 6.53 ; max = 24.7
ΔE*ab: mean = 16.8 ; max = 29.7
sRGB (D65)
b*
a*
100
80
60
40
20
0
-20
-40
-60
-60
-40
-20
0
20
40
60
80
1
2
3
4
5
6
7
8
9
10
11
12
13
14
15
16
17
18

FIG. 12

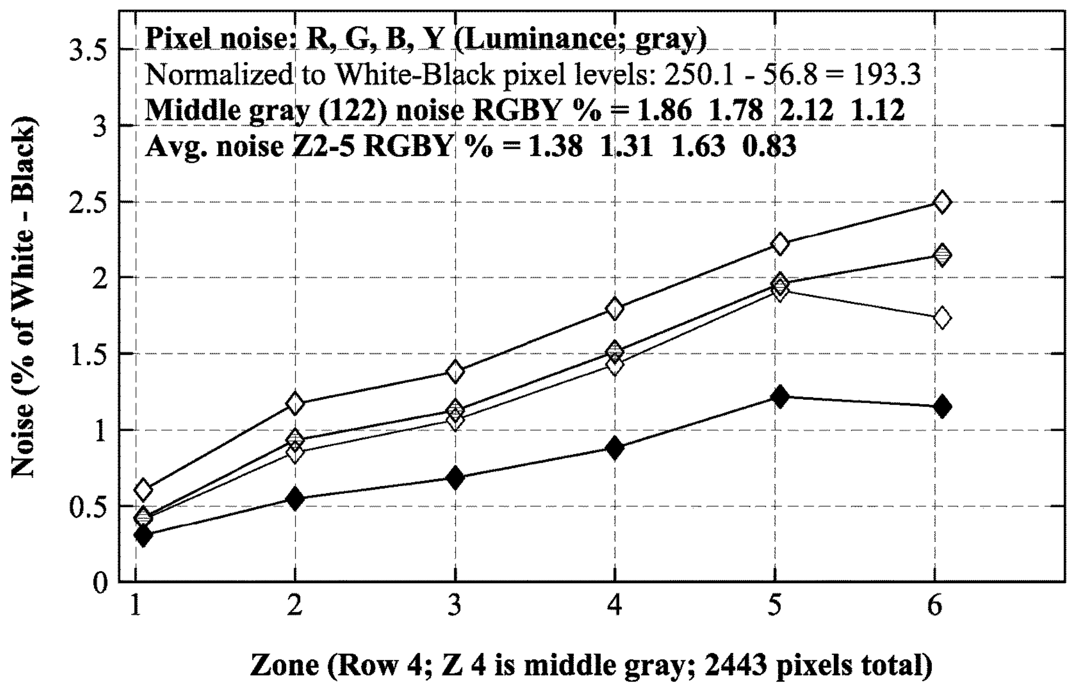
Pixel noise: R, G, B, Y (Luminance; gray)
Normalized to White-Black pixel levels: 250.1 - 56.8 = 193.3
Middle gray (122) noise RGBY % = 1.86 1.78 2.12 1.12
Avg. noise Z2-5 RGBY % = 1.38 1.31 1.63 0.83
Noise (% of White - Black)
3.5
3
2.5
2
1.5
1
0.5
0
1
2
3
4
5
6
Zone (Row 4; Z 4 is middle gray; 2443 pixels total)

FIG. 13

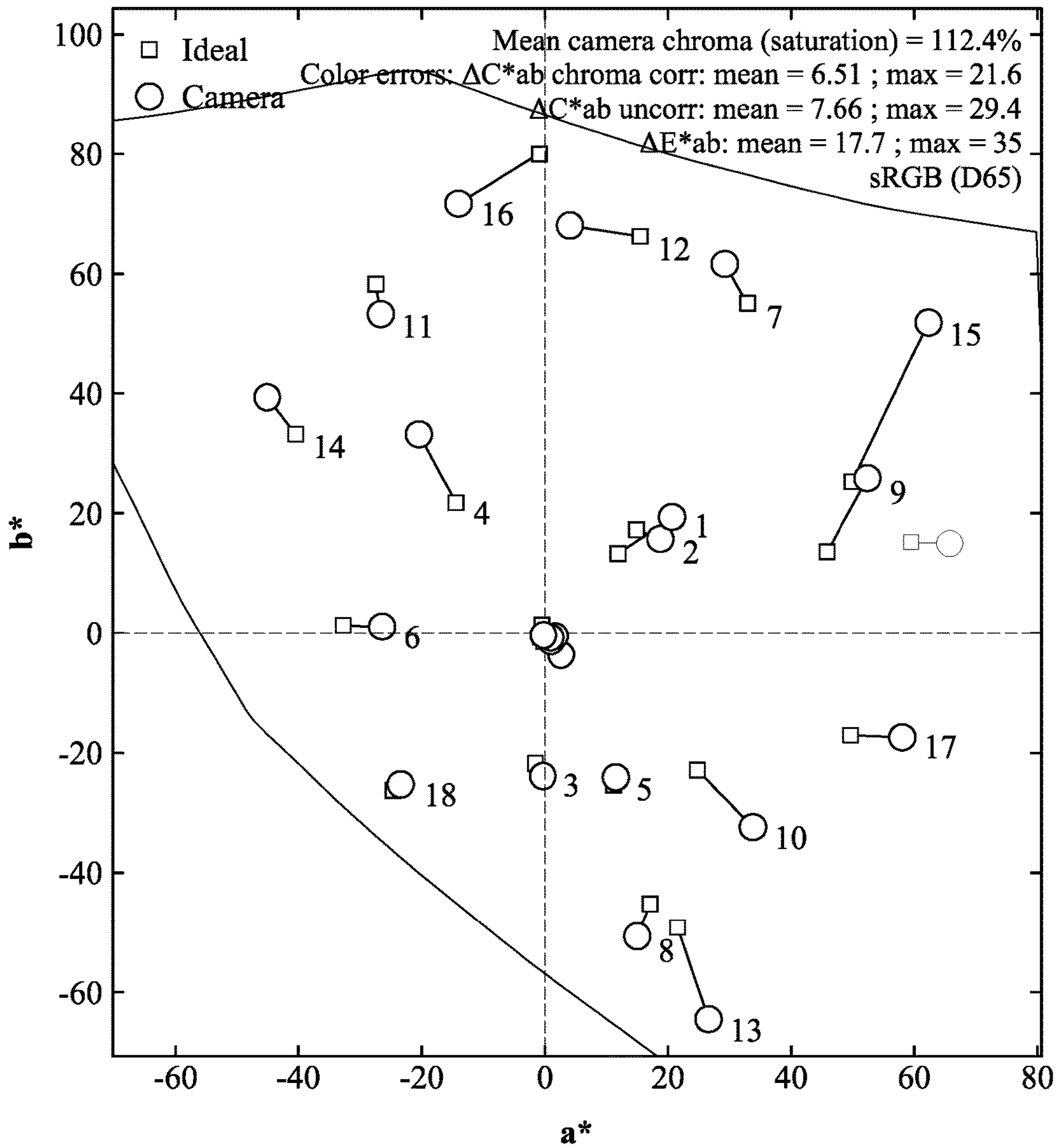
Ideal
Camera
Mean camera chroma (saturation) = 112.4%
Color errors: ΔC*ab chroma corr: mean = 6.51 ; max = 21.6
ΔC*ab uncorr: mean = 7.66 ; max = 29.4
ΔE*ab: mean = 17.7 ; max = 35
sRGB (D65)
b*
a*
100
80
60
40
20
0
-20
-40
-60
-60
-40
-20
0
20
40
60
80
1
2
3
4
5
6
7
8
9
10
11
12
13
14
15
16
17
18

FIG. 14

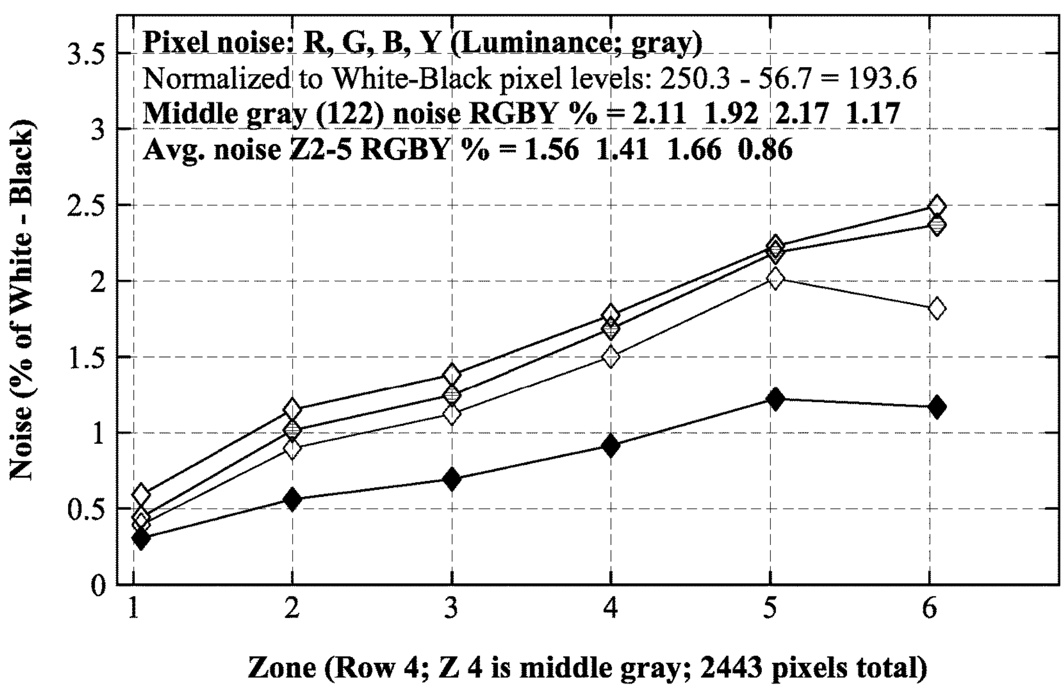
Pixel noise: R, G, B, Y (Luminance; gray)
Normalized to White-Black pixel levels: 250.3 - 56.7 = 193.6
Middle gray (122) noise RGBY % = 2.11 1.92 2.17 1.17
Avg. noise Z2-5 RGBY % = 1.56 1.41 1.66 0.86
Noise (% of White - Black)
3.5
3
2.5
2
1.5
1
0.5
0
1
2
3
4
5
6
Zone (Row 4; Z 4 is middle gray; 2443 pixels total)

FIG. 15

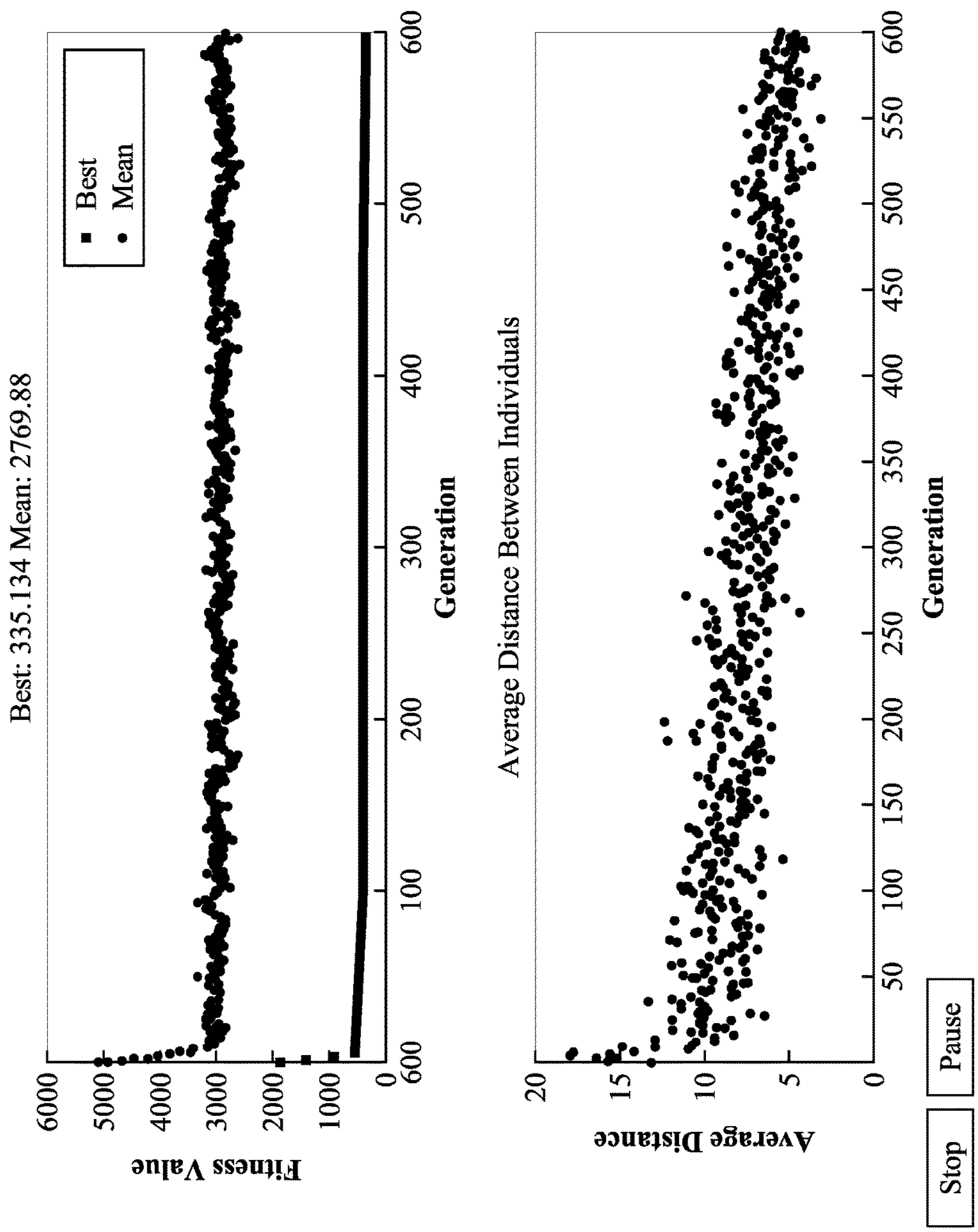
Best: 335.134 Mean: 2769.88
Best
Mean
Fitness Value
6000
5000
4000
3000
2000
1000
0
Generation
600
100
200
300
400
500
600
Average Distance Between Individuals
Average Distance
20
15
10
5
0
Generation
50
100
150
200
250
300
350
400
450
500
550
600
Stop
Pause

FIG. 16

COLOR CORRECTION SYSTEM AND METHOD

CROSS-REFERENCE TO RELATED APPLICATIONS

This application is a continuation of, and claims priority to, copending PCT Patent Application Number PCT/CN2015/079094, which was filed on May 15, 2015. The disclosure of the PCT application is herein incorporated by reference in its entirety and for all purposes.

COPYRIGHT NOTICE

FIELD

The disclosed embodiments relate generally to digital image processing and more particularly, but not exclusively, to systems and methods for color correction of digital images.

BACKGROUND

Because digital imaging devices acquire colors differently from the way that human eyes perceive color, images acquired by digital imaging devices typically benefit from color correction. However, the color correction process may be prone to introducing and/or amplifying different types of noise. This is the general area that embodiments of the invention are intended to address.

BRIEF DESCRIPTION OF THE DRAWINGS

FIG. **1** is an exemplary top-level block diagram illustrating an embodiment of a color correction apparatus for color-correcting a digital image.

FIG. **2** is an exemplary diagram illustrating an embodiment of an imaging system including the color correction apparatus of FIG. **1**, wherein the imaging system is shown imaging a color reference using an image sensor.

FIG. **3** is an exemplary diagram illustrating an alternative embodiment of the imaging system of FIG. **2**, wherein the color correction apparatus is shown as acquiring various color values for calibration of color correction parameters.

FIG. **4** is exemplary top-level flow chart illustrating an embodiment of a method for calibrating a digital imaging device.

FIG. **5** is exemplary flow chart illustrating an alternative embodiment of the method of FIG. **4**, wherein color correction parameters are optimized for calibrating a digital imaging device.

FIG. **6** is exemplary flow chart illustrating an alternative embodiment of the method of FIG. **5**, wherein the method includes a two-step optimization method.

FIG. **7** is exemplary flow chart illustrating another alternative embodiment of the method of FIG. **5**, wherein the method includes a genetic process.

FIG. **8** is an exemplary diagram illustrating an embodiment of the method of FIG. **5**, wherein the method includes sampling at different spatial frequencies to determine a noise amplification metric.

FIG. **9** is an exemplary diagram illustrating an embodiment of the method of FIG. **8** with spatial downsampling.

FIG. **10** is an exemplary flow chart illustrating an embodiment of the method of FIG. **5**, wherein the method includes sampling at different spatial frequencies to determine a noise amplification metric.

FIG. **11** is an exemplary diagram illustrating an embodiment of an imaging system installed on an unmanned aerial vehicle (UAV).

FIG. **12** is an exemplary diagram illustrating a chrominance diagram showing a color error of a first experiment testing the efficacy of optimizing color correction parameters with noise regulation.

FIG. **13** is an exemplary diagram illustrating noise values of the experiment of FIG. **9** testing the efficacy of optimizing color correction parameters with noise regulation.

FIG. **14** is an exemplary diagram illustrating a chrominance diagram showing a color error of a second experiment testing the efficacy of optimizing color correction parameters without noise regulation.

FIG. **15** is an exemplary diagram illustrating noise values of the experiment of FIG. **11** testing the efficacy of optimizing color correction parameters without noise regulation.

FIG. **16** is an exemplary diagram illustrating a two-step method for optimizing color correction parameters with noise regulation.

It should be noted that the figures are not drawn to scale and that elements of similar structures or functions are generally represented by like reference numerals for illustrative purposes throughout the figures. It also should be noted that the figures are only intended to facilitate the description of the preferred embodiments. The figures do not illustrate every aspect of the described embodiments and do not limit the scope of the present disclosure.

DETAILED DESCRIPTION OF THE PREFERRED EMBODIMENTS

The invention is illustrated, by way of example and not by way of limitation, in the figures of the accompanying drawings in which like references indicate similar elements. It should be noted that references to “an” or “one” or “some” embodiment(s) in this disclosure are not necessarily to the same embodiment, and such references mean at least one.

Color correction is a process that transforms signals acquired by photosensors of digital imaging devices into colors that look realistic. Color correction is a transformation defined by a set of color correction parameters. These parameters are typically calibrated for each individual digital imaging device to find customized parameter values that accurately reflect the color response characteristics of the individual device.

The calibration of color correction parameters entails an optimization process in which colors values acquired by the imaging device are compared with known reference color values. Typically, the goal during the optimization process is to minimize a difference between the acquired colors post-color-correction and the known reference values. A drawback of this approach, however, is that accounting for color correction accuracy alone can often result in parameters that excessively amplify noise. Image noise can include color and brightness variations in an image. These variations are not features of an original object imaged but, instead, are attributable to artifacts introduced by the acquisition and processing of the image. Sources of noise include, for example, quantum exposure noise, dark current noise, thermal noise, readout noise, and others. Since image noise is inversely proportional to the size of the imaging device, the problem of noise is especially acute for smaller imaging devices. When image acquisition is performed aboard mobile platforms such as unmanned aerial vehicles (UAVs), the image noise problem is especially acute both because of the smaller cameras used on the mobile platforms and because of noise introduced by movement of the mobile platforms. In view of the foregoing, there is a need for improved color correction systems and methods that increase color correction accuracy while limiting noise amplification.

The present disclosure sets forth systems and methods for color correction of a digital image which overcome shortcomings of existing color correction techniques by increasing color correction accuracy while limiting noise amplification. Based on color reference images, color correction parameters are calibrated to increase color correction accuracy while limiting noise amplification. The calibration can be performed in the CIE L*a*b* color space to more closely reflect human perception of distances between colors. The calibration can be performed with reference to a virtual noisy image that can be sampled at different spatial frequencies. At each spatial frequency, a peak signal-to-noise ratio (PSNR) can be used to evaluate the amount of noise introduced by color correction. The color correction parameters can be optimized by using a genetic process. A two-step parameter optimization method can be used that avoid the optimization process being trapped in local optima. The present systems and methods advantageously are suitable for use, for example, by unmanned aerial vehicles (UAVs) and other mobile platforms.

Turning now to FIG. **1**, an exemplary color correction apparatus **100** is shown as including a processor **110** and a memory **120**. The processor **110** can comprise any type of processing system. Exemplary processors **110** can include, without limitation, one or more general purpose microprocessors (for example, single or multi-core processors), application-specific integrated circuits, application-specific instruction-set processors, graphics processing units, physics processing units, digital signal processing units, coprocessors, network processing units, audio processing units, encryption processing units, and the like. In certain embodiments, the processor **110** can include an image processing engine or media processing unit, which can include specialized hardware for enhancing the speed and efficiency of certain operations for image capture, image filtering, and image processing. Such operations include, for example, Bayer transformations, demosaicing operations, white balancing operations, color correction operations, noise reduction operations, and/or image sharpening/softening operations. In certain embodiments, the processor **110** can include specialized hardware and/or software for performing various color correction parameter calibration functions and operations described herein. Specialized hardware can include, but are not limited to, specialized parallel processors, caches, high speed buses, and the like.

The memory **120** can comprise any type of memory and can be, for example, a random access memory (RAM), a static RAM, a dynamic RAM, a read-only memory (ROM), a programmable ROM, an erasable programmable ROM, an electrically erasable programmable ROM, a flash memory, a secure digital (SD) card, and the like. Preferably, the memory **120** has a storage capacity that accommodates the needs of the color correction parameter calibration functions and operations described herein. The memory **120** can have any commercially-available memory capacity suitable for use in image processing applications and preferably has a storage capacity of at least 512 Megabytes, 1 Gigabyte, 2 Gigabytes, 4 Gigabytes, 16 Gigabytes, 32 Gigabytes, 64 Gigabytes, or more. In some embodiments, the memory **120** can be a non-transitory storage medium that can store instructions for performing any of the processes described herein.

The color correction apparatus **100** can further include any hardware and/or software desired for performing the color correction parameter calibration functions and operations described herein. For example, the color correction apparatus **100** can include one or more input/output interfaces (not shown). Exemplary interfaces include, but are not limited to, universal serial bus (USB), digital visual interface (DVI), display port, serial ATA (SATA), IEEE 1394 interface (also known as FireWire), serial, video graphics array (VGA), super video graphics array (SVGA), small computer system interface (SCSI), high-definition multimedia interface (HDMI), audio ports, and/or proprietary input/output interfaces. As another example, the color correction apparatus **100** can include one or more input/output devices (not shown), for example, buttons, a keyboard, keypad, trackball, displays, and/or a monitor. As yet another example, the color correction apparatus **100** can include hardware for communication between components of the color correction apparatus **100** (for example, between the processor **110** and the memory **120**).

Turning now to FIG. **2**, an exemplary embodiment of an imaging system **200** is shown as including a color correction apparatus **100**, an image sensor **130**, and a color filter **140**. The color correction apparatus **100** can be provided in the manner discussed in more detail above with reference to FIG. **1**. The memory **120** of the color correction apparatus **100** is shown as storing color correction parameters **125**, noise generation parameters **126**, pre-correction and post-correction image data **127**, and intermediate values **128** produced during various color correction parameter calibration functions and operations described herein. The image sensor **130** can perform the function of sensing light and converting the sensed light into electrical signals that can be rendered as an image. Various image sensors **130** are suitable for use with the disclosed systems and methods, including, but not limited to, image sensors **130** used in commercially-available cameras and camcorders. Suitable image sensors **130** can include analog image sensors (for example, video camera tubes) and/or digital image sensors (for example, charge-coupled device (CCD), complementary metal-oxide-semiconductor (CMOS), N-type metal-oxide-semiconductor (NMOS) image sensors, and hybrids/variants thereof). Digital image sensors can include, for example, a two-dimensional array of photosensor elements that can each capture one pixel of image information. The resolution of the image sensor **130** can be determined by the number of photosensor elements. The image sensor **130** can support any commercially-available image resolution and preferably has a resolution of at least 0.1 Megapixels, 0.5 Megapixels, 1 Megapixel, 2 Megapixels, 5 Megapixels, 10 Megapixels, or an even greater number of pixels. The image sensor **130** can have specialty functions for use in various applications such as thermography, creation of multi-spectral images, infrared detection, gamma detection, x-ray detection, and the like. The image sensor **130** can include, for example, an electro-optical sensor, a thermal/infrared sensor, a color or monochrome sensor, a multi-spectral imaging sensor, a spectrophotometer, a spectrometer, a thermometer, and/or an illuminometer.

The color filter **140** is shown in FIG. **2** as separating and/or filtering incoming light based on color and directing the light onto the appropriate photosensor elements of the image sensor **130**. For example, the color filter **140** can include a color filter array that passes red, green, or blue light to selected pixel sensors to form a color mosaic (not shown). The layout of different colors on the color mosaic can be arranged in any convenient manner, including a Bayer pattern. Once a color mosaic is formed, a color value of each pixel can be interpolated using any of various demosaicing methods that interpolate missing color values at each pixel using color values of adjacent pixels. As an alternative to filtering and demosaicing, the image sensor **130** can include an array of layered pixel photosensor elements that separates light of different wavelengths based on the properties of the photosensor elements. In either case, an image can be acquired by the image sensor **130** as intensity values in each of a plurality of color channels at each pixel.

The imaging system **200** is further shown in FIG. **2** as acquiring an image of a color reference **150** to perform calibration of color correction parameters **125**. The color reference **150** preferably has a known reference color value C_{ref} that is known or that can be otherwise determined in advance, making the color reference **150** suitable for use as a color standard. Stated somewhat differently, the reference color value C_{ref} is a property of the color reference **150** that is independent of how the color reference **150** is imaged. The reference color value C_{ref} can be designated based on an average human perception of the color reference **150**. The reference color value C_{ref} can thus serve as an objective measure how a color imaged by the image sensor **130** can be corrected so as to match the average human perception.

The color reference **150** is preferably, but not necessarily, homogeneous in color. Flatness of the color reference **150** is preferable, though not essential, to avoid variations attributable to differential light scattering. The optical properties of the color reference **150** need not be ideal for purposes of performing color correction, so long as the optical properties do not interfere with imaging the color reference **150**. The color reference **150** can be made of one or more of a variety of materials such as plastic, paper, metal, wood, foam, composites thereof, and other materials. Furthermore, the color, reflectance, and/or other optical properties of the color reference **150** can advantageously be calibrated as desired using an appropriate paint or other coating. In some embodiments, the color reference **150** can advantageously include multiple color patches **151**, each of which has a different reference color value C_{ref}. This embodiment enables multiple color references **150** to be imaged at the same time, reducing the number of image capture operations for color correction. This embodiment is particularly suitable when a large number of color references **150** are to be imaged in order to calibrate color correction parameters **125** with greater accuracy. Commercially available color references **150** include, for example, MacBeth ColorChecker, MacBeth ColorChecker SG, and the like.

Although images acquired by the image sensor **130** are described above in an RGB (red, green, and blue) color space for illustrative purposes only, the images can be acquired in other color spaces, as well. The color space in which images are acquired depends generally on the properties of the image sensor **130** and any color filters **140**. Furthermore, the color space in which an image is acquired need not be three-dimensional but can have any number of dimensions as desired to capture the spectral composition of the image. The number of dimensions can depend on the number of color channels of the image sensor **130**. The color space of an acquired image can be one-dimensional, two-dimensional, three-dimensional, four-dimensional, five-dimensional, or more.

Once acquired by the image sensor **130**, an image can be converted between color spaces as desired for processing and/or calibration. For example, a conversion from a sRGB color space with coordinates (R_{sRGB}, G_{sRGB}, B_{sRGB}) to a CIE 1931 XYZ color space with coordinates (X, Y, Z) entails a linear conversion, which can be represented by the following three-dimensional matrix:

$$\begin{bmatrix} X \\ Y \\ Z \end{bmatrix} = \begin{bmatrix} 0.4124 & 0.3576 & 0.1805 \\ 0.2126 & 0.7152 & 0.0722 \\ 0.0193 & 0.1192 & 0.9505 \end{bmatrix} \begin{bmatrix} R_{sRGB} \\ G_{sRGB} \\ B_{sRGB} \end{bmatrix} \quad \text{Equation (1)}$$

In some embodiments, it can be desirable to express the color of an image in a non-linear color space. One suitable non-linear color space for imaging applications is a CIE L*a*b* color space (for example, a CIE 1976 L*a*b* color space) as defined by the International Commission on Illumination. The color of an image in a CIE L*a*b* color space can be computed from the colors of the image in a CIE 1931 XYZ color space using the following non-linear transformation:

$$L^* = 116f\left(\frac{Y}{Y_n}\right) - 16 \quad \text{Equation (2)}$$

$$a^* = 500\left[f\left(\frac{X}{X_n}\right) - f\left(\frac{Y}{Y_n}\right)\right] \quad \text{Equation (3)}$$

$$b^* = 200\left[f\left(\frac{Y}{Y_n}\right) - f\left(\frac{Z}{Z_n}\right)\right] \quad \text{Equation (4)}$$

$$\text{where } f(t) = \begin{cases} t^{1/3} & \text{if } t > \left(\frac{6}{29}\right)^3 \\ \frac{1}{3}\left(\frac{29}{6}\right)^2 t + \frac{4}{29} & \text{otherwise} \end{cases} \quad \text{Equation (5)}$$

In the above equations (2)-(5), X_n, Y_n, and Z_n are the CIE XYZ values of the color at a reference white point. The CIE L*a*b* color space is designed to mimic the color response of human perception. The non-linearity of the transformation from the CIE XYZ color space to the CIE L*a*b* color space reflects the nonlinearity of human perception. Representing a color in the CIE L*a*b* color space has the advantage that the CIE L*a*b* color space is perceptually uniform to human beings, meaning that a change of a given amount in a color value will produce a proportional change of visual significance. According, calibration of color correction parameters **125** can advantageously be performed after converting input and reference colors into a CIE L*a*b* color space representation.

In some embodiments, it can be desirable to express the color of an image in a YUV color space (for example, a Y'UV color space). The YUV color space is represented by one luminance component Y representing image brightness and two chrominance components U and V representing image color. A conversion from a RGB color space with coordinates (R, G, B) to a YUV color space with coordinates

(Y, U, V) entails a linear conversion, which can be represented by the following three-dimensional matrix:

$$\begin{bmatrix} Y \\ U \\ V \end{bmatrix} = \begin{bmatrix} 0.299 & 0.587 & 0.114 \\ -0.14713 & -0.28886 & 0.436 \\ 0.615 & -0.51499 & -0.10001 \end{bmatrix} \begin{bmatrix} G \\ B \\ R \end{bmatrix} \quad \text{Equation (6)}$$

Although conversions between specific color spaces are shown and described for illustrative purposes only, an image can be converted from any first predetermined color space to any other second predetermined color space as desired.

Turning now to FIG. **3**, an alternative embodiment of the imaging system **200** is shown. The imaging system **200** of FIG. **3** includes a color correction apparatus **100**, which is shown as obtaining several inputs for calibration of color correction parameters **125**. Without limitation, an image sensor **130** is shown as acquiring an image of a color reference **150**. The image is then passed to the color correction apparatus **100**, which can obtain an input color value C_{in} of the image. The input color value C_{in} represents a pre-color-corrected value that reflects the image acquisition properties of the image sensor **130**, filtering properties of an image filter **140**, as well as any other optical properties of the imaging system **200**. In one embodiment, the input color value C_{in} can be transformed from the color space of the color reference image to a non-linear color space—for example, a CIE L*a*b* color space. The transformation can be performed, for example, by first using a linear transformation from a RGB color space to an intermediate CIE XYZ color using Equation (1) shown above. The color values in the intermediate CIE XYZ color space can be non-linearly transformed to a CIE L*a*b* color space as shown above in Equations (2)-(5). Such transformations can be performed on a processor **110** (shown in FIG. **1**) of the color correction apparatus **100**.

Similarly, the color correction apparatus **100** can obtain a reference color value C_{ref} that corresponds to the input color value C_{in} for color reference **150**. If desired, the reference color value C_{ref} can be transformed into a non-linear color space—for example, the CIE L*a*b* color space. In some embodiments, the reference color value C_{ref} advantageously can be directly inputted into the color correction apparatus **100** in the CIE L*a*b* color space, thereby making the transformation step unnecessary.

In FIG. **3**, the color correction apparatus **100** is further shown as obtaining noise evaluation color values C_{noise} from a noise evaluation image **160**. The noise evaluation image **160** can be any image containing noise. As color correction tends to amplify noise, the noise evaluation image **160** can be used to calibrate color correction parameters **125** in order to limit noise amplification. Stated somewhat differently, the noise evaluation image **160** can used to evaluate now noise is amplified with a given set of color correction parameters **125** (shown in FIG. **2**), and thereby select a set of color correction parameters **125** with reduced noise amplification. In one embodiment, the noise evaluation color values C_{noise} can be transformed into the YUV color space, as further described below with reference to FIG. **7**. The transformation can be performed, for example, using the linear transformation from the RGB color space to the YUV color space shown above in Equation (6). This transformation can be performed using the processor **110** of the color correction apparatus **100**.

In one embodiment, the noise evaluation image **160** can be an image acquired by the image sensor **130** with or without filtering through the color filter **140**. In this embodiment, the noise evaluation image **160** is preferably an image of the color reference **150**. Imaging the color reference **150** advantageous allows the simultaneous determination of the input color values C_{in} and the noise evaluation color values C_{noise}.

Alternatively and/or additionally, the noise evaluation image **160** can be a virtual noise evaluation image **160**A. The virtual noise evaluation image **160**A can be generated by the color correction apparatus **100** using a pre-determined set of noise generation parameters **126** (shown in FIG. **2**). The noise generation parameters **126** can, for example, reflect the distribution of the noise that is generated virtually (for example, Poisson or Gaussian noise). The specific noise generation parameters **126** can reflect the types of noise that the imaging system **200** can be expected to encounter in usage. A virtual noise evaluation image **160**A can be used because the evaluation of noise amplification does not require information about the color of an underlying object that is imaged. Instead, an arbitrary image containing noise can be evaluated for how the noise of that image would be amplified under a given set of color correction parameters **125**. For example, the noise evaluation color values C_{noise} of the virtual noise evaluation image **160**A can be represented as follows:

$$C_{noise} = C_{noise\_free} \pm n \quad \text{Equation (7)}$$

where C_{noise_free} represents the color of the virtual noise evaluation image **160**A before noise is added, and n represents the noise added.

Once the inputs for color correction parameter calibration (for example, input color values C_{in}, reference color values C_{ref}, and noise evaluation color values C_{noise}) are obtained by the color correction apparatus **100**, these inputs can be stored for later use by the color correction apparatus **100** (for example, in a memory **120** as shown in FIG. **1**). For example, the inputs for color correction parameter calibration can be obtained as part of an initialization process for a new imaging device **200** prior to usage. The inputs for color correction parameter calibration can be stored in the memory **120** and called upon periodically to re-calibrate the color correction parameters **125** as desired (for example, as image response characteristics of the imaging device **200** change after wear and tear). The inputs for color correction parameter calibration can be, but do not need to be, re-obtained for each new color correction parameter calibration.

Turning now to FIG. **4**, an exemplary top-level method **400** of calibrating color correction parameters **125** is shown. The method **400** advantageously can be applied to calibrating the color correction parameters **125** for a digital imaging device **200** (shown in FIGS. **2** and **3**). At **401**, input color values C_{in} and reference color values C_{ref} are obtained for each of a plurality of color references **150** (shown in FIGS. **2** and **3**). Preferably, the input color values C_{in} and reference color values C_{ref} are obtained or transformed into a non-linear color space—for example, a CIE L*a*b* color space—as described above with reference to FIG. **3**. Additionally, a noise evaluation image **160** having a color noise for evaluating noise reduction is obtained.

At **402**, a plurality of color correction parameters **125** are adjusted so as to optimize a fitness function J. In some embodiments, the fitness function J can comprise a color correction error e_{color} and/or a noise amplification metric D_{noise} based on the input color values C_{in}, the reference color values C_{ref}, and the noise evaluation image **160**. An exemplary embodiment of the adjusting is described in more detail below with respect to FIG. **5**.

Turning now to FIG. **5**, an exemplary method **500** of calibrating color correction parameters **125** (shown in FIG. **2**) for a digital imaging device **200** (shown in FIGS. **2** and **3**) is shown. At **501**, input color (or pre-correction) values C_{in} for a color references **150** are color corrected using the current values of the color correction parameters **125** to obtain post-correction input color values $\hat{C}_{in}$. This operation can be represented as:

$$\hat{C}_{in}=CC(C_{in}) \quad \text{Equation (8)}$$

In the above equation (8), CC represents a color correction operation. The specific implementation of the color correction operation CC depends on the underlying form of the color correction parameters **125**. In one embodiment, the color correction parameters **125** can take the form of a matrix having dimensions n×m, where m is dimensionality of the pre-correction color value and n is the dimensionality of the post-correction color value. In this embodiment, the color correction operation CC will take the form of a matrix multiplication that transforms an m-dimensional color value vector into an n-dimensional color value vector. Preferably, the pre-correction color value and the post-correction color value have the same dimensionality, in which case CC will take the form of a square matrix. Preferably, the pre-correction color value and the post-correction color value are each three-dimensional (for example, for color values in the RGB, CIE XYZ, CIE L*a*b*, and LUV color spaces), in which case CC will take the form of a 3×3 matrix. An advantage of using a matrix is that a matrix can describe a color correction operation CC using only n×m correction parameters **125**, allowing decreased memory usage. However, linear color correction using a matrix may be unsuitable for some applications.

In another embodiment, the color correction parameters **125** can take the form of a look-up table (LUT) indexed in m dimensions that contains ordered m-tuples $(a_1, a_2, \ldots, a_m)$ each mapping to an n-dimensional vector, where m is dimensionality of the pre-correction color value and n is the dimensionality of the post-correction color value. Preferably, the look-up table is three-dimensional, that is, indexed in three dimensions. An advantage of using a look-up table to implement the color correction parameters **125** is that a look-up table can account for a non-linear relationship between a pre-correction color value and a post-correction color value. Furthermore, since the entries in the look-up table are discrete, interpolation operations can be performed when pre-correction color values fall in between discrete entries. Such interpolation operations can include finding look-up table entries that have the closest distance (for example, Euclidian distance) to the pre-correction color value, and interpolating a corrected color value using the closest look-up table entries. For example, linear interpolations can be performed for one-dimensional look-up tables, and multi-linear interpolations can be performed for look-up tables in higher dimensions. In this embodiment, the color correction operation CC will take the form of a look-up operation in the look-up table, followed by an interpolation operation, if desired. The color correction parameters **125** can be implemented in multiple ways simultaneously; for example, a combination of a matrix and a look-up table can be used.

In one embodiment, a Shepard interpolation can be used to perform color correction where the color correction parameters **125** take the form of a look-up table (LUT). In one embodiment, a color-corrected value for a given color p can be found as follows:

$$f(p) = \frac{\sum_{i=1}^{n} \hat{f}(c_i) w_i(\|p - c_i\|)}{\sum_{i=1}^{n} w_i(\|p - c_i\|)} \quad \text{Equation (9)}$$

In the above equation (9), i is an index over the different input color values C_{in} and their corresponding reference color values C_{ref}, c_i represents the ith value of the input color values C_{in}, $\hat{f}(c_i)$ represents the ith value of the reference color values C_{ref}, $(\|p-c_i\|)$ represents a distance (for example, a Euclidian distance) between the given color p and c_i, and w_i represents a weight of the ith input color value C_{in}.

At **502**, the post-correction input color values $\hat{C}_{in}$ are compared with the reference color values C_{ref}, and the color correction error e_{color} is computed based on the comparison. For example, where the post-correction input color values $\hat{C}_{in}$ and reference color values C_{ref} are represented in a CIE L*a*b* color space, the color correction error e_{cozor} can be expressed as:

$$e_{color} = \sqrt{\sum_{j}^{j \in \{L^*, a^*, b^*\}} \left(C_{in\_j} - \hat{C}_{in\_j}\right)^2} \quad \text{Equation (10)}$$

In the above equation (10), C_{in_j} and $\hat{C}_{in\_j}$ represent the jth component of the reference color values C_{ref} and the post-correction input color values $\hat{C}_{in}$, respectively. Stated somewhat differently, the color correction error e_{color} is the Euclidian distance between the post-correction input color values $\hat{C}_{in}$ and the reference color values Cretin the color space in which the color values are represented. Where the color correction error e_{color} is to be determined over multiple color references **150** (or, equivalently, over multiple color patches **151** of a given color reference **150**), the color correction error e_{color} can be taken as a weighted and/or unweighted average over the color patches **151**.

At **503**, noise evaluation color values C_{noise} are color corrected using the current values of the color correction parameters **125** to obtain post-correction noise evaluation color values $\hat{C}_{noise}$. This operation can be represented as:

$$\hat{C}_{noise}=CC(C_{noise}) \quad \text{Equation (11)}$$

In the above equation (11), CC represents a color correction operation as described above with reference to **501**. The specific color correction operation CC depends on the implementation of the color correction parameters **125** and, as described above with reference to **501**, can take the form of a matrix or a look-up table with each form having respective advantages.

At **504**, the post-correction noise evaluation color values $\hat{C}_{noise}$ are compared with pre-correction noise evaluation color values C_{noise}, and the noise amplification metric D_{noise} is found based on the comparison. The noise amplification metric D_{noise} can be any measure of the distance between post-correction noise evaluation color values $\hat{C}_{noise}$ and the pre-correction noise evaluation color values C_{noise}. That is, the greater the value of the noise amplification metric D_{noise}, the more noise is amplified after applying a color correction.

Where the noise amplification metric D_{noise} is to be determined over multiple color references **150** (or, equivalently, over multiple color patches **151** of a given color reference **150**), the noise amplification metric D_{noise} can be taken as a weighted and/or unweighted average over the color patches **151**. In one embodiment, the noise amplification metric D_{noise} can be taken as a weighted average over the color patches **151**.

$$D_{noise} = \frac{\sum_{i=1}^{N} \omega_i D_i}{\sum_{i=1}^{N} \omega_i} \quad \text{Equation (12)}$$

In the above equation (12), i is an index over the color patches **151**, N is the total number of color patches **151**, D_i is the noise amplification metric for color patch i, and ω_i, is a non-negative weight for color patch i. The weights ω_i can be set according to the sensitivity of the average human perception to the color of each color patch **151**. For example, colors having greater sensitivity of human perception can be given greater weights ω_i.

At **505**, a fitness function J can be determined. In some embodiments, the fitness function J can be found as a weighted and/or unweighted sum of the color correction error e_{color} and the noise amplification metric D_{noise}. For example, an unweighted fitness function J can be represented as the following sum:

$$J = e_{color} + D_{noise} \quad \text{Equation (13)}$$

In some embodiments, a weighted fitness function J can used to advantageously weight the color correction error e_{color} more than the noise amplification metric D_{noise}, or vice versa. The amount of weighting for the fitness function J can be determined, for example, by repeating a color correction parameter calibrations for different weights and taking the weight that gives the best (for example, the lowest) value of the fitness function J. Alternatively and/or additionally, the amount of weighting for the fitness function J can be determined based on prior color correction parameter calibrations (for example, using different imaging devices).

Turning now to FIG. **6**, an exemplary method **600** for calibrating color correction parameters **125** (shown in FIG. **2**) is shown as including two steps. At **601**, a first optimization process is applied to obtain initial values CC_0 for the color correction parameters **125**. The first optimization preferably samples broadly the space of possible color correction parameter values so as to avoid becoming trapped in local optima. Any of various optimization processes can be used in the first optimization at **601**, including a genetic process, a simulated annealing method, and other non-greedy methods that avoid local optima. At **602**, a second optimization process is applied using the initial values CC_0 as a starting point to obtain further optimized values CC_{opt} for the color correction parameters **125**. At the second optimization, at **602**, a goal is to find the local optimum value. Accordingly, direct optimization methods are suitable for the second optimization at **602**. Exemplary direct optimization methods include, but are not limited to, gradient descent methods.

Turning now to FIG. **7**, an exemplary genetic process **700** is shown for calibrating color correction parameters **125** (shown in FIG. **2**). A genetic process is an optimization method loosely based on evolutionary principles in biology, where possible solutions to a problem are generated as members of a "population," and the members are selected based on a fitness function over a number of selection rounds. The genetic process **700** can be used to find an optimal solution to the problem of selecting a set of color correction parameters **125** to optimize (for example, minimize) the fitness function J that includes a color correction error e_{color} and a noise amplification metric D_{noise}. At **701**, a predetermined number N of initial sets of candidate color correction parameters **125**A are selected as the initial "population" of solutions. The predetermined number N can comprise any suitable number of initial sets and, for example, can be at least 10, 50, 100, 500, 1000, or more. The initial population of the N sets of candidate color correction parameters **125**A can be selected, for example, by sampling the space of possible parameters at specified intervals. Alternatively and/or additionally, the sampling can be done at random.

At **702**, the fitness function J is evaluated for the members of the "population," that is, for each of the N sets of candidate color correction parameters **125**A. From among the N initial sets of candidate color correction parameters **125**A, the initial set that has the best value of the fitness function J (for example, the minimal value, if the fitness function J to be minimized) is chosen. At **703**, if the best value passes a predefined threshold, the genetic process stops at **704**. Alternatively and/or additionally, at **705**, if certain conditions are met (for example, the genetic process has been run for more than a certain number of rounds, or the genetic process has not produced more than a specific amount of improvement in the fitness function J from the prior round), the genetic process stops at **704**. After the genetic process stops, at **704**, the candidate color correction parameters **125**A giving the best value of the fitness function J is declared to be the "winner," and these candidate color correction parameters **125**A can be outputted and/or used as a starting point for further optimization.

If the "best" candidate correction parameters **125** do not pass a predefined threshold and/or certain conditions for stopping the genetic process, at **703**, are not met, the genetic process continues, at **706**, by discarding and replacing candidate color correction parameters **125**A having the lowest values of the fitness function J. In one embodiment, a given percentile of the candidate color correction parameters **125**A having the lowest fitness function J can be discarded and replaced with new candidate color correction parameters **125**A. The new candidate color correction parameters **125**A can, for example, be generated in the same way as the initial candidate color correction parameters **125**A. In some embodiments, at least 10%, 20%, 30%, 40%, 50%, or more the lowest scoring fitness functions J can be discarded.

At **707**, "mutation" operations can be applied to the candidate color correction parameters **125**A, simulating biological mutations of chromosomes between successive generations of individuals. Here, each set of candidate color correction parameters **125**A can be conceptually treated as a "chromosome" that is also subject to mutation. Mutations to the candidate color correction parameters **125**A include, for example, "point mutations" changing individual parameters at random and/or "crossover" mutations between two sets of candidate color correction parameters **125**A. For example, where the candidate color correction parameters **125**A take the form of a matrix, a crossover can be performed by swapping corresponding rows and/or columns or portions thereof between two candidate matrices. Where the candidate color correction parameters **125**A take the form of a look-up table, a crossover can be performed by swapping one or more corresponding entries in the look-up table. Once the mutations are applied to the candidate color correction parameters **125**A, the method **700** can return to **702** for evaluating the fitness function J for the new round of the genetic process.

The noise amplification metric D_{noise} can be determined using any suitable approach, including but not limited to using peak signal-to-noise ratios (PSNR) and/or color variances.

Turning now to FIG. **8**, an exemplary diagram is shown for finding the noise amplification metric D_{noise} using a peak signal-to-noise ratios (PSNR). Beginning with noise-free color values C_{noise_free}, noise-evaluation color values C_{noise} can be found by adding noise n, as described in Equation (7). A color correction CC can be applied to the noise-free color values C_{noise_free} and noise-evaluation color values C_{noise}, respectively, to find corresponding post-correction values of the noise-free color values $\ddot{C}_{noise\_free}$ and noise evaluation color values $\hat{C}_{noise}$. For example, the color correction is shown in Equation (11) and in Equation (14) below:

$$C_{noise\_free}=CC(C_{nosie\_free}) \quad \text{Equation (14)}$$

Based on the parameters C_{noise_free}, C_{noise}, $\hat{C}_{noise\_free}$, and $\hat{C}_{noise}$, a pair of PSNR values PSNR and $\widehat{PSNR}$ can be found through determining a mean squared error (MSE), as shown in Equations (15) through (18):

$$MSE = \frac{\|c_{noise} - c_{noise\_free}\|_2^2}{\Sigma_j s_j} \quad \text{Equation (15)}$$

$$PSNR = 10\log_{10}\left(\frac{\text{MAX}_I^2}{MSE}\right) \quad \text{Equation (16)}$$

In the above equations (15)-(16), S, i.e. $\Sigma_j S_j$, is the number of pixels and MAX_I is the maximum value of C_{noise} and C_{noise_free}, and j is an index over virtual color patches.

$$\widehat{MSE} = \frac{\|\hat{c}_{noise} - \hat{c}_{noise\_free}\|_2^2}{\Sigma_j s_j} \quad \text{Equation (17)}$$

$$\widehat{PSNR} = 10\log_{10}\left(\frac{\text{MAX}_I^2}{\widehat{MSE}}\right) \quad \text{Equation (18)}$$

In the above equations (17)-(18), S, i.e. $\Sigma_j S_j$, is the number of pixels and MAX_I is the maximum value of $\hat{C}_{noise}$ and $\hat{C}_{noise\_free}$, and/is an index over virtual color patches

In some embodiments, determining the noise amplification metric D_{noise} can include finding a PSNR difference that is a difference between a PSNR for the pre-correction noise evaluation image and a $\widehat{PSNR}$ for the corrected noise evaluation image.

In some embodiments, the noise amplification metric D_{noise} can be determined by downsampling. For example, the downsampling can be a spatial downsampling, as illustrated in FIG. **9**. In particular, FIG. **9** illustrates an embodiment of downsampling in which an image (for example, images having pre-correction noise evaluation color values C_{noise}, or pre-correction noise-free color values C_{noise_free}) is sample at every other pixel in a first downsampling. In some embodiments, the downsampled image can be downsampling again, and the downsampling process can be repeated as often as desired up to M iterations. Although not shown in FIG. **9**, a similar downsampling process can be performed for images that have been color-corrected (for example, images having post-correction noise evaluation color values $\hat{C}_{noise}$ or post-correction noise-free color values $\hat{C}_{noise\_free}$). Since downsampling can be an iterative process, color values and PSNR values at particular iterations are denoted with a subscript from 0 to M corresponding to the iteration, as shown in FIGS. **8**-**9**.

After each round of downsampling, the downsampled images can be used to determine one or more downsampled PSNRs as well as a downsampled PSNR difference. Returning to FIG. **8**, pre-correction noise-free color values $C_{noise\_free_1}$ and pre-correction noise evaluation color values C_{noise_1} that have undergone one round of downsampling can be used to find a corresponding downsampled $PSNR_1$. Likewise, post-correction noise-free color values $\hat{C}_{noise\_free_1}$ and post-correction noise evaluation color values $\hat{C}_{noise_1}$ that have undergone one round of downsampling can be used to find a corresponding downsampled $\widehat{PSNR}_i$. After M downsampling rounds, a set of PSNR values $PSNR_i$ and $\widehat{PSNR}_i$ will be obtained, where i ranges from 0 to M. The set of PSNR values can be used to find corresponding PSNR differences for value of i ranging from 0 to M, where i=0 corresponds to a PSNR difference that has not been downsampled, and i=m corresponds to a PSNR difference that has been downsampled m times.

In some embodiments, the noise amplification metric D_{noise} can be obtained by taking a weighted average of a PSNR difference and at least one downsampled PSNR difference. In some embodiments, the noise amplification metric D_{noise} can be obtained by taking a weighted average of the PSNR difference and the plurality of successively downsampled PSNR differences. The weight applied to each PSNR difference and/or downsampled PSNR difference can represented as w_i, where i ranges from 0 to M. An exemplary method of finding the noise amplification metric D_{noise} is shown as follows in Equation (19), which is reproduced in FIG. **8**:

$$D_{noise} = \frac{\sum_{i=0}^{M} w_i(PSNR_i - \widehat{PSNR}_i)}{\sum_{i=0}^{M} w_i} \quad \text{Equation (19)}$$

where M is the total number of downsampling iterations and w_i is the weight given to each downsampling iteration i.

In some embodiments, at least one of the weights w_i is non-zero. Stated somewhat differently, PSNR differences at one or more iterations i can be given a weight of zero to effectively ignore that PSNR difference, provided that not all of the weights are ignored.

Turning now to FIG. **10**, an exemplary method **1000** is shown for finding the noise amplification metric D_{noise} that locates and compares peak signal-to-noise ratios (PSNR) at successively downsampled frequencies. At **1001***a*, an initial value of a pre-correction PSNR $PSNR_0$ can be found using the pre-correction noise evaluation color values C_{noise_0} and pre-correction noise-free color values $C_{noise\_free_0}$, as described above with reference to FIGS. **8** and **9**. At **1002***a*, C_{noise_0} and $C_{noise\_free_0}$ can each be downsampled to obtain C_{noise_1} and $C_{noise\_free_1}$, respectively. At **1003***a*, a downsampled $PSNR_i$ can be found from C_{noisei} and $C_{noise\_free_1}$. Optionally, at **1004***a*, the process of downsampling and finding a corresponding downsampled PSNR can be repeated for M iterations, as desired.

Similarly, the iterative downsampling process can be repeated for color-corrected images. At **1001***b*, an initial value of a post-correction PSNR $\widehat{PSNR}_0$ can be found using the post-correction noise evaluation color values $\hat{C}_{noise_0}$ and post-correction noise-free color values $\hat{C}_{noise\_free_0}$, as described above with reference to FIGS. **8** and **9**. At **1002***b*, $\hat{C}_{noise_0}$ and $\hat{C}_{noise\_free_0}$ can each be downsampled to obtain $\hat{C}_{noise_1}$ and $\hat{C}_{noise\_free_1}$, respectively. At **1003***b*, a downsampled $\widehat{PSNR}_1$ can be found from $\hat{C}_{noise_1}$ and $\hat{C}_{noise\_free_1}$. Optionally, at **1004***b*, the process of downsampling and finding a corresponding downsampled $\widehat{PSNR}$ can be repeated for M iterations, as desired.

Finally, at **1005**, the set of PSNR values and color-corrected PSNR values found at iterations 0 to M can be used to find the noise amplification metric D_{noise}—for example, as shown above in Equation (19).

In another embodiment, the noise amplification metric D_{noise} can be obtained based on a variance of Y, U, and V components of the pre-correction noise evaluation color values C_{noise_0} and post-correction noise evaluation color values $\hat{C}_{noise_0}$. In an exemplary embodiment, the noise amplification metric D_{noise} can be obtained using the Equation (20):

$$D_{noisy} = \frac{\sum_{i=0}^{M} w_i \left(\frac{\mathrm{Var}_{noisy_{Y_i}}}{\mathrm{Var}_{noise\_input_{Y_i}}} + \frac{\mathrm{Var}_{noisy_{U_i}}}{\mathrm{Var}_{noise\_input_{U_i}}} + \frac{\mathrm{Var}_{noisy_{V_i}}}{\mathrm{Var}_{noise\_input_{U_i}}} \right)}{\sum_{i=0}^{M} w_i} \qquad \text{Equation (20)}$$

wherein

$$\mathrm{Var}_{noise\_input_{Y_i}}$$

represents the variance of the Y components of the pre-correction noise evaluation color values

$$C_{noise_i}, \text{ and } \mathrm{Var}_{noisy_{Y_i}}$$

represents the variance of the Y components of the post-correction noise evaluation color values $\hat{C}_{noise_i}$, and likewise for the U and V components, and w_i is the weight given to each downsampling iteration i, where $w_i \geq 0$.

Turning now to FIG. **11**, an exemplary embodiment of the imaging system **200** is shown wherein the imaging system **200** is shown as being installed aboard an unmanned aerial vehicle (UAV) **1100**. A UAV **1100**, colloquially referred to as a "drone," is an aircraft without an onboard human pilot and whose flight is controlled autonomously and/or by a remote pilot. The imaging system **200** is suitable for installation aboard any of various types of UAVs **1100**, including, but not limited to, rotocraft, fixed-wing aircraft, and hybrids thereof. Suitable rotocraft include, for example, single rotor, dual rotor, trirotor, quadrotor (quadcopter), hexarotor, and octorotor rotocraft. The imaging system **200** can be installed on various portions of the UAV **1100**. For example, the imaging system **200** can be installed within a fuselage **1110** of the UAV **1100**. Alternatively, the imaging system **200** can be mounted onto an exterior surface **1020** (for example, on the underside **1025**) of the UAV **1100**. Furthermore, the various components of the imaging system **200** can be installed on the same portion, and/or different portions, of the UAV **1100**. For example, an image sensor **130** can be mounted on an exterior surface **1120** to facilitate image acquisition; while, a color correction apparatus **100** advantageously can be installed within the fuselage **1110** for protection against wear and tear. Likewise, the various components of the color correction apparatus **100** can be installed on the same portion, and/or different portions, of the UAV **1100**. Although shown and described with respect to a UAV **1100** for purposes of illustration only, the imaging system **200** can include, or be mounted on, any type of mobile platform. Exemplary suitable mobile platforms include, but are not limited to, bicycles, automobiles, trucks, ships, boats, trains, helicopters, aircraft, various hybrids thereof, and the like.

EXAMPLE 1

The following color correction parameter calibration experiment was performed to determine the efficacy of a method of calibration with noise regulation in comparison to the method without noise regulation. First, an input image was used to calibrate color correction parameters by using a fitness function that includes the noise amplification metric in the manner described above. FIG. **12** shows a chrominance diagram of resulting color errors in a CIE L*a*b* color space (showing a cross section in the a* and b* dimensions), showing a mean color correction error of 16.8 with a maximum color correction error of 29.7. FIG. **13** shows a plot of the resulting noise levels from the same experiment, showing that the average Y (luminance) noise is 0.83%; while, the average chrominance noise in the R, G, and B components are 1.38%, 1.31%, and 1.63%, respectively.

In contrast, the same input image was used to calibrate color correction parameters by using a fitness function that does not include the noise amplification metric. FIG. **14** shows a chrominance diagram of resulting color errors in a CIE L*a*b* color space, showing a mean color correction error of 17.7 with a maximum color correction error of 35, both of which are significantly greater than the corresponding errors obtained with noise regulation. FIG. **15** shows a plot of the corresponding noise levels of the experiment, showing that the average Y (luminance) noise is 0.86%; while, the average chrominance noise in the R, G, and B components are 1.56%, 1.31%, and 1.66%, respectively, which are significantly greater than the noise obtained by calibration with noise regulation. Accordingly, it can be seen from this experiment that color correction parameter calibration with noise regulation is an improvement over color correction parameter calibration without noise regulation.

EXAMPLE 2

The following color correction parameter calibration experiment was performed to determine the efficacy of a method of calibration with conversion to a CIE L*a*b* color space in comparison to the method that performs the calibration in a CIE XYZ color space. First, an input image was used to calibrate color correction parameters after the input and reference colors of the input image are converted to a CIE L*a*b*. Optimization yielded the following matrix of color correction parameters:

$$M_1 = \begin{bmatrix} 0.47009134530394125 & 0.30369624777814247 & 0.226212406917916 \\ 0.1126102415 & 0.5888365492340442 & 0.29855320919654277 \\ 0.07360346735208151 & -0.258973359 & 1.1853698917599211 \end{bmatrix}$$

having an optimized e_c of 2.412169304.

Next, the same input image was used to calibrate color correction parameters after the input and reference colors of the input image are converted to a CIE XYZ. Optimization yielded the following matrix of color correction parameters:

$$M_2 = \begin{bmatrix} 1.11570755070485 & 0.160204597011795 & 0.044497 \\ -0.473878528884461 & 1.60653254387421 & -0.132654014989749 \\ -0.0543893885667206 & -0.8115292 & 1.86591858820061 \end{bmatrix}$$

having an optimized e_c of 3.0107447. This comparison shows that using a non-linear color space—here, a CIE L*a*b* color space—yields improved results over using a CIE XYZ color space.

EXAMPLE 3

The following example shows the process of optimizing a set of color correction parameters using the two-step method of FIG. **6**. In the first step of the two-step method, a genetic process is used to find a set of initial parameters so as to avoid becoming trapped in local optima. The fitness value of the parameters for the genetic process over six hundred generations is shown in FIG. **16** at the upper panel, showing that the fitness value reaches a best value of 335.134 after 600 generations. In the second step of the two-step method, a direct optimization process is used starting from the initial parameters produced at the end of step one. In the second step, after another 600 generations, the direct optimization method reduces the average distance between the corrected input colors and the corresponding reference colors, as shown in FIG. **15** at the lower panel. This example shows that it is advantageous to use a two-step optimization method.

The disclosed embodiments are susceptible to various modifications and alternative forms, and specific examples thereof have been shown by way of example in the drawings and are herein described in detail. It should be understood, however, that the disclosed embodiments are not to be limited to the particular forms or methods disclosed, but to the contrary, the disclosed embodiments are to cover all modifications, equivalents, and alternatives.

What is claimed is:

1. A method for calibrating a digital imaging device for color correction, comprising:

obtaining input color values and reference color values for respective color references, the input color values and reference color values being in a non-linear color space;

obtaining a noise evaluation image having a color noise for evaluating noise reduction; and

adjusting a plurality of color correction parameters based on the input color values, reference color values, and the noise evaluation image using a fitness function, having a color correction error and a noise amplification metric, wherein said adjusting comprises determining the noise amplification metric by:

color correcting the noise evaluation image using the color correction parameters; and

comparing the corrected noise evaluation image with the pre-correction noise evaluation image.

2. The method of claim **1**, wherein said obtaining the input color values comprises imaging the color references each having a plurality of color patches.

3. The method of claim **1**, wherein said obtaining the noise evaluation image comprises obtaining a virtual noise evaluation image.

4. The method of claim **1**, wherein said adjusting comprises determining the color correction error by:

color correcting the input color values; and

comparing the corrected input color values with the reference color values.

5. The method of claim **1**, wherein said determining the noise amplification metric comprises determining the noise amplification metric using a peak signal-to-noise ratio (PSNR).

6. The method of claim **5**, wherein said determining the noise amplification metric comprises finding a PSNR difference that is a difference between a PSNR for the pre-correction noise evaluation image and a PSNR for the corrected noise evaluation image.

7. The method of claim **6**, wherein said determining the noise amplification metric comprises determining a downsampled PSNR difference by:

downsampling the pre-correction noise evaluation image to obtain a downsampled pre-correction noise evaluation image;

downsampling the corrected noise evaluation image to obtain a downsampled corrected noise evaluation image; and

finding the downsampled PSNR difference as a difference between a PSNR for the downsampled pre-correction noise evaluation image and a PSNR for the downsampled corrected noise evaluation image.

8. The method of claim **1**, wherein said determining the noise amplification metric comprises determining the noise amplification metric by converting the color corrected noise evaluation image into a YUV color space.

9. The method of claim **1**, further comprising determining the noise amplification metric as a weighted sum of noise amplification levels of each of a plurality of color patches of the noise evaluation image.

10. The method of claim **1**, wherein said adjusting the color correction parameters comprises performing look-up operations and interpolation operations in a look-up table.

11. The method of claim **10**, wherein said adjusting the color correction parameters comprises performing an interpolation operation that is a Shepard interpolation.

12. An apparatus, comprising:

a processor configured to:

receive input color values and reference color values for respective color references, the input color values and reference color values being in a non-linear color space;

receive a noise evaluation image having a color noise for evaluating noise reduction; and

adjust a plurality of color correction parameters based on the input color values, reference color values, and the noise evaluation image using a fitness function having a color correction error and a noise amplification metric, wherein said adjusting comprises determining the noise amplification metric by:

color correcting the noise evaluation image using the color correction parameters; and

comparing the corrected noise evaluation image with the pre-correction noise evaluation image.

13. The apparatus of claim **12**, wherein said processor is configured to determine the color correction error by:

color correcting the input color values; and

comparing the corrected input color values with the reference color values.

14. The apparatus of claim **12**, wherein said processor is configured to determine the noise amplification metric using a peak signal-to-noise ratio (PSNR).

15. The apparatus of claim **14**, wherein said processor is configured to determine the noise amplification metric by finding a PSNR difference that is a difference between a PSNR for the pre-correction noise evaluation image and a PSNR for the corrected noise evaluation image.

16. The apparatus of claim **15**, wherein said processor is configured to determine the noise amplification metric by determining a downsampled PSNR difference by:

downsampling the pre-correction noise evaluation image to obtain a downsampled pre-correction noise evaluation image;

downsampling the corrected noise evaluation image to obtain a downsampled corrected noise evaluation image; and

finding the downsampled PSNR difference as a difference between a PSNR for the downsampled pre-correction noise evaluation image and a PSNR for the downsampled corrected noise evaluation image.

17. The apparatus of claim **12**, wherein the noise evaluation image comprises a plurality of color patches, and wherein the noise amplification metric is determined as a weighted sum of noise amplification levels of each of the color patches.

18. The apparatus of claim **12**, wherein the apparatus is mounted aboard an unmanned aerial vehicle (UAV).

19. The apparatus of claims **12**, wherein said determining the noise amplification metric comprises determining the noise amplification metric by converting the color corrected noise evaluation image into a YUV color space.

20. The apparatus of claims **12**, wherein said adjusting the color correction parameters comprises performing look-up operations and interpolation operations in a look-up table.

21. An imaging device, comprising:

an image sensor for imaging a plurality of color references; and

a processor configured to:

receive input color values and reference color values for respective color references, the input color values and reference color values being in a non-linear color space;

receive a noise evaluation image having a color noise for evaluating noise reduction; and

adjust a plurality of color correction parameters based on the input color values, reference color values, and the noise evaluation image using a fitness having a color correction error and a noise amplification metric, wherein said adjusting comprises determining the noise amplification metric by:

color correcting the noise evaluation image using the color correction parameters; and

comparing the corrected noise evaluation image with the pre-correction noise evaluation image.

22. The imaging device of claims **21**, wherein the imaging device is mounted aboard an unmanned aerial vehicle (UAV).

23. The imaging device of claims **21**, wherein the processor is configured to determine the noise amplification metric as a weighted sum of noise amplification levels of each of a plurality of color patches of the noise evaluation image.

24. The imaging device of claims **21**, wherein said processor is configured to determine the noise amplification metric using a peak signal-to-noise ratio (PSNR).

25. A non-transitory readable medium with instructions stored thereon that, when executed by a processor, perform the steps comprising:

obtaining input color values and reference color values for respective color references, the input color values and reference color values being in a non-linear color space;

obtaining a noise evaluation image having a color noise for evaluating noise reduction; and

adjusting a plurality of color correction parameters based on the input color values, reference color values, and the noise evaluation image using a fitness having a color correction error and a noise amplification metric, wherein said adjusting comprises determining the noise amplification metric by:

color correcting the noise evaluation image using the color correction parameters; and

comparing the corrected noise evaluation image with the pre-correction noise evaluation image.

26. The non-transitory readable medium of claim **25**, wherein said adjusting comprises determining the color correction error by:

color correcting the input color values; and

comparing the corrected input color values with the reference color values.

27. The non-transitory readable medium of claim **25**, wherein said determining the noise amplification metric comprises determining the noise amplification metric using a peak signal-to-noise ratio (PSNR).

28. The non-transitory readable medium of claim **27**, wherein said determining the noise amplification metric comprises finding a PSNR difference that is a difference between a PSNR for the pre-correction noise evaluation image and a PSNR for the corrected noise evaluation image.

29. The non-transitory readable medium of claim **25**, wherein said steps further comprise determining the noise amplification metric as a weighted sum of noise amplification levels of each of a plurality of color patches of the noise evaluation image.

30. The non-transitory readable medium of claim **25**, wherein said determining the noise amplification metric comprises determining a downsampled PSNR difference by:

downsampling the pre-correction noise evaluation image to obtain a downsampled pre-correction noise evaluation image;

downsampling the corrected noise evaluation image to obtain a downsampled corrected noise evaluation image; and

finding the downsampled PSNR difference as a difference between a PSNR for the downsampled pre-correction noise evaluation image and a PSNR for the downsampled corrected noise evaluation image.

* * * * *